The Holocene

Vegetation changes and plant wax biomarkers from an ombrotrophic bog define hydroclimate trends and human-environment interactions during the Holocene in northern Norway

Journal:	*The Holocene*
Manuscript ID	HOL-20-0002.R2
Manuscript Type:	Paper
Date Submitted by the Author:	n/a
Complete List of Authors:	Balascio, Nicholas; College of William & Mary, Geology Anderson, R.; Northern Arizona University, CESE; D'Andrea, William; Columbia University, Lamont-Doherty Earth Observatory Wickler, Stephen; UiT The Arctic University of Norway The Arctic University Museum of Norway D'Andrea, Robert; Northern Arizona University Bakke, Jostein; University of Bergen, Dept of Earth sciene
Keywords:	Holocene, Peat bog, Pollen, Plant wax biomarkers, Norway, Hydroclimate, Paleoclimate, coprophilous fungi
Abstract:	Holocene climate records from northern Europe improve our understanding of important North Atlantic ocean and atmospheric circulation systems to long-term insolation-driven changes, as well as more rapid forcing and feedback mechanisms. Here we assess Holocene climate and environmental changes in northern Norway based on the analysis of pollen, non-pollen palynomorphs, plant macrofossils, and plant wax biomarkers from a high latitude ombrotrophic bog. We define the extent and thickness of Hollabåttjønnen Bog (0.16 km^2), which is located 10 km north of Tromsø. Several cores were analyzed, including a 5.16-m core that spans the last 9.5 cal ka BP. Vegetation changes from several sites were reconstructed and the distribution and hydrogen isotopic composition (δD) of *n*-alkanes (C_{21}-C_{33}) were analyzed. Our data show several distinct climate intervals that primarily indicate changes in bog surface moisture. In the early Holocene (c. 9.5-7.7 cal ka BP), wetter conditions are defined by the presence of wetland sedges and grasses, higher concentrations of mid-chain length *n*-alkanes, and a similarity in δD values among homologs. A dry mid-Holocene (c. 7.7-3.8 cal ka BP) is inferred from the presence of a heath shrubland, low peat accumulations rates, and significant differences between δD values of mid- and long-chain length *n*-alkanes. The late Holocene (c. 3.8 cal ka BP-present) is marked by the onset of wetter conditions, lateral bog expansion, and an increase in sedges and grasses. The Hollabåttjønnen Bog record is also significant because its margins were an important location for human settlement. We correlate early Holocene

	environmental conditions with changes in Stone Age structures recently excavated, and we identify the occurrence of coprophilous fungi, such as *Sporormiella* and *Sordaria*, likely associated with reindeer grazing activity beginning c. 1 cal ka BP. This site therefore provides important regional paleoclimate information as well as context for evaluating local prehistoric human-environment interactions.

Vegetation changes and plant wax biomarkers from an ombrotrophic bog define hydroclimate trends and human-environment interactions during the Holocene in northern Norway

Nicholas L. Balascio[1*], R. Scott Anderson[2], William J. D'Andrea[3], Stephen Wickler[4], Robert M. D'Andrea[2], Jostein Bakke[5]

[1] *Department of Geology, The College of William & Mary, Williamsburg, VA 23187*
[2] *School of Earth & Environmental Sustainability, Northern Arizona University, Flagstaff, AZ 86011*
[3]*Lamont-Doherty Earth Observatory of Columbia University, Palisades, NY 10964*
[4] *The Arctic University Museum of Norway, UiT The Arctic University of Norway, NO-9037 Tromsø, Norway*
[5] *Department of Earth Science, University of Bergen, N-5007 Bergen, Norway*

*Corresponding author e-mail: nbalascio@wm.edu

Abstract

Holocene climate records from northern Europe improve our understanding of important North Atlantic ocean and atmospheric circulation systems to long-term insolation-driven changes, as well as more rapid forcing and feedback mechanisms. Here we assess Holocene climate and environmental changes in northern Norway based on the analysis of pollen, non-pollen palynomorphs, plant macrofossils, and plant wax biomarkers from a high latitude ombrotrophic bog. We define the extent and thickness of Hollabåttjønnen Bog (0.16 km^2), which is located 10 km north of Tromsø. Several cores were analyzed, including a 5.16-m core that spans the last 9.5 cal ka BP. Vegetation changes from several sites were reconstructed and the distribution and hydrogen isotopic composition (δD) of *n*-alkanes (C_{21}-C_{33}) were analyzed. Our data show several distinct climate intervals that primarily indicate changes in bog surface moisture. In the early Holocene (c. 9.5-7.7 cal ka BP), wetter conditions are defined by the presence of wetland sedges and grasses, higher concentrations of mid-chain length *n*-alkanes, and a similarity in δD values among homologs. A dry mid-Holocene (c. 7.7-3.8 cal ka BP) is inferred from the presence of a heath shrubland, low peat accumulations rates, and significant differences between δD values of mid- and long-chain length *n*-alkanes. The late Holocene (c. 3.8 cal ka BP-present) is marked by the onset of wetter conditions, lateral bog expansion, and an increase in sedges and grasses. The Hollabåttjønnen Bog record is also significant because its margins were an important location for human settlement. We correlate early Holocene environmental conditions with changes in Stone Age structures recently excavated, and we identify the occurrence of coprophilous fungi, such as *Sporormiella* and *Sordaria*, likely associated with reindeer grazing activity beginning c. 1 cal ka BP. This site therefore provides important regional paleoclimate information as well as context for evaluating local prehistoric human-environment interactions.

Introduction

Holocene paleoclimate records provide a long-term perspective on present climate trends (Battarbee and Binney, 2008). They allow us to analyze how environmental systems respond to forcing and feedback mechanisms, as well as to examine the interactions between climate and human activities over different timescales (Oldfield, 2008). In northern Norway, millennial-scale Holocene climate trends are primarily forced by orbital-driven changes in northern hemisphere summer insolation and the response of North Atlantic atmospheric and oceanic circulation systems (Eldevik et al., 2014; Sejrup et al., 2016). Marine and terrestrial paleoclimate records in northern Fennoscandia show distinct characteristics that broadly define early, mid-, and late Holocene intervals (Calvo et al., 2002; Risebrobakken et al., 2003, 2010; Nesje et al., 2005, 2008; Hald et al., 2007; Jansen et al., 2008; Seppä et al., 2009; Eldevik et al., 2014; Sejrup et al., 2016). Generally, the early Holocene is marked by an overall warming trend in sea-surface and atmospheric temperatures and the recession of mountain glaciers, punctuated by periodic cooling events. A maximum in sea surface and atmospheric temperatures defines the mid-Holocene when most glaciers in Norway completely melted, and was followed by colder temperatures and the re-advance of mountain glaciers during the late Holocene. Evidence for hydroclimate changes corresponding to these intervals has also been documented by pollen data, lake level records, and glacier reconstructions (e.g. Eronen et al., 1999; Bakke et al., 2008; Bjune and Birks, 2008). Despite our knowledge of these general climate trends, more information is needed to understand the impact of paleoclimate and paleoenvironmental changes on a regional scale and at higher resolution. Moreover, concurrent with climate changes during the Holocene was the spread of people throughout northern Fennoscandia in the early Holocene and the establishment of permanent settlements during the late Holocene (Bjerk, 2008; Balbo et al. 2010; Möller et al., 2012; Breivik, 2014; Glørstad, 2014; Rowley-Conwy and Piper, 2016; Balascio and Wickler, 2018). Improved paleoenvironmental analysis can further contextualize these developments and better evaluate the scale of human-environment interactions.

In this study we developed a record of local Holocene climate and environmental change from Hollabåttjønnen Bog, an ombrotrophic bog in northern Norway (Figure 1). Peatlands are important environments that contain a variety of paleoenvironmental data in Arctic and sub-Arctic regions (Barber, 2006; Charman et al., 2009; Amesbury et al., 2012). We apply an integrated approach to assessing the bog stratigraphy by analyzing pollen, non-pollen palynomorphs (NPPs), plant macrofossils, and plant wax biomarkers to develop a comprehensive understanding of vegetation and hydrologic changes. This site is significant not only because a ~5 m thick peat developed during the Holocene suitable for paleoenvironmental analysis (Balascio and Anderson, 2014), but also because the margins of the bog were an important location for human settlement dating back to c. 9,500 cal yr BP (Gjerde and Hole, 2013; Gjerde and Skandfer, 2017) and recently the subject of extensive archaeological study (Skandfer et al., 2010; Gjerde and Hole, 2013; Nergaard et al., 2016). In addition to the pollen, we recovered spores of both *Sporormiella* and *Sordaria*, coprophilous fungi recording the presence of herbivore-use of the bog surface. This paleoenvironmental analysis not only provides a better understanding of the impact of Holocene climate changes on this region, but also an evaluation of environmental conditions relevant to the history of local human activity.

Peatlands as records of environmental change

Peatlands are common throughout northern Europe from oceanic to more continental localities. They are important environmental systems because they are archives of vegetation changes recorded by pollen and macrofossils, they have a role in sequestering carbon, and they are sensitive to climate changes (Barber, 2006). Ombrotrophic peatlands, bogs fed only from direct rainfall, are of particular interest because their development and surface moisture content is related to local climate, primarily seasonal precipitation and evaporation (Barber, 1993). Reconstructing bog surface moisture conditions therefore can provide important paleoclimate information (Charman et al., 2009).

The actual relationship between the moisture content of a bog and climate is complex. The influence of precipitation and temperature on bog surface moisture has been investigated from numerous sites in northern Europe from oceanic to continental regions and they generally show a greater influence of temperature (precipitation) at more continental (oceanic) sites, although this relationship is not always consistent (as reviewed by Amesbury et al., 2012). Summer temperatures are also typically negatively correlated with precipitation so disentangling the influence of either parameter is difficult (Charman et al., 2009; Amesbury et al., 2012). However, at oceanic sites in western Europe, changes in bog surface wetness have been associated with the strength and location of the westerlies (Charman et al., 2009). In northern Norway, there are a few studies that have reconstructed bog surface wetness (Vorren et al., 2007; Nichols et al., 2009; Vorren et al., 2012). Vorren et al. (2012) identify a series of wet intervals during the Holocene and Nichols et al. (2009) document changes in moisture conditions and the seasonality of precipitation, which they also attribute to changes in the strength of atmospheric circulation delivering precipitation to the region.

Methods for reconstructing bog surface moisture conditions have primarily included the analysis of pollen and plant macrofossils (Barber et al., 1994), peat humification (Aaby, 1976; Blackford and Chamber, 1991, 1993, Chamber et al., 1997; Vorren et al., 2007, 2012), and testate amoebae (Warner and Charman, 1994; Woodland et al., 1998; Charman, 1999). More recently, organic biomarker proxies have also been shown to provide a range of paleoenvironmental information from ombrotrophic bogs (Nott et al., 2000; Pancost et al., 2002; Nichols et al., 2006, 2009, 2014). In this study, we analyzed environmental conditions using pollen, NPPs, plant macrofossils, and plant wax biomarkers (*n*-alkanes). Pollen and plant macrofossils are directly related to local vegetation changes and alkane distributions provide further information on characteristics of vegetation changes (Nott et al., 2000; Pancost et al., 2002; Diefendorf et al., 2011; Bush and McInerney, 2013, Diefendorf et al., 2015). NPPs are "extra" microfossils (sensu van Geel, 2001), including fungi, protozoa, algae and others that can inform on human activities and paleoenvironmental conditions. Mid- and long-chain length *n*-alkanes (C_{21}-C_{33}) are produced by peat-forming mosses and plants and their distributions are influenced by vegetation changes and bog hydrology (Nott et al., 2000; Pancost et al., 2002; Nichols et al., 2006). Changes in the composition of peatlands through time can therefore be interpreted using metrics such as the average chain length (ACL) of *n*-alkanes (Poynter et al., 1989). If more detail is known about the chain-length characteristics of dominant vegetation types at a site, specific interpretations can also be made about compositional changes. For example, in some environments *Sphagnum* has been shown to have higher concentrations of mid-chain length *n*-alkanes, while vascular plants typically have higher concentrations of long-chain length *n*-alkanes (Baas et a., 2000; Pancost et al., 2002; Nichols et al., 2006). The *Sphagnum*/Vascular Ratio (SVR) quantifies changes in n-C_{23} relative to n-C_{29} and represents a comparison of the amount of *Sphagnum*-derived alkanes relative to vascular plant-derived alkanes (Nichols et al., 2006). In addition, hydrogen isotope values of *n*-alkanes reflect source water used by plants after modification during biosynthesis (apparent fractionation) and can be used to infer changes in available water and regional rainfall characteristics (Sachse et al., 2012; Kahmen et al., 2013a,b). Precipitation isotopes are influenced by factors related to the hydrologic cycle and regional climatology (Bowen and Revenaugh, 2003). In the North Atlantic region, climate is strongly influenced by the northward transport of heat associated with the North Atlantic Current as well as interaction between polar and mid-latitude air masses. During the Holocene, precipitation isotope changes were most likely affected by variations in the strength of ocean heat transport and its influence on air mass trajectories that resulted in isotopic differences in moisture delivered from local versus regional sources (Balascio et al., 2018b; Curtin et al., 2019). The isotopic composition of water available to bog plants is determined by local precipitation, but can also vary for plants with and without vascular systems that access water from the rooting zone (acrotelm) and bog surface, respectively, which can experience differences in evaporation (Nichols et al., 2010).

Study area

The Hollabåttjønnen Bog (69°44.47'N, 19°7.55'E; 24-29 m a.s.l.; 0.16 km^2) is located 6 km north of Tromsø on the Skarpeneset Peninsula near Tønsnes, Norway (Figure 1). The region experiences a relatively mild climate despite its high latitude location. Mean annual temperatures are 3°C with a mean annual precipitation of 1020 mm. The bog formed on a Lateglacial recessional moraine deposited by the Balsfjord glacier during the Skarpnes event, c. 14.5-14.0 cal ka BP (Vorren and Plassen, 2002). The moraine extends out into the fjord and therefore the bog is ombrotrophic, fed only by rain and snowmelt on the bog surface with no groundwater or surface water influence from the adjacent hillside. The bog surface is hummocky with several ponds, ~5 m in diameter, and covers an area of 0.1 km^2 (Figure 1).

Modern vegetation

Modern mire vegetation in this area has been extensively studied by Vorren et al. (1999) who analyzed 303 relevés from mires in Troms and Norland counties. These sites were oriented immediately north and south of 69°N from c. 19°40'E to 15°46' E. Hollabåttjønnen Bog in Tønsnes is contained within this cluster of relevés, near the northern boundary. Vegetation on Hollabåttjønnen Bog includes: subshrub specimens of *Betula nana* (dvergbjørk, dwarf birch), *Rubus chamaemorus* (molte, cloudberry), *Empetrum nigrum* (krekling, crowberry), *Vaccinium vitis-idaea* (tyttebær, bear berry), *Andromeda polifolia* (hvitlyng, andromeda), *Salix reticulata* (rynkevier, netleaf willow) and *Chamaepericlymenum suecicum* (skrubb-bær, bunchberry). Also common are *Eriophorum* cf. *scheuchzeri* (snømyrull, Scheuchzers cottongrass) and *E*. cf. *vaginatum* (torvmyrull, tussock cottongrass), with *Euphrasia* cf. *wettsteinii* (fjelløyentrøst, eyebright), *Juncus* sp. (Sivfamilien, rush) and mosses and locally common *Drosera rotundifolia* (rundsoldogg, sundew) (nomenclature after Mossberg and Stenberg 2010). *Betula pubescens* (bjørk, European white birch) grows on uplands and well-drained sites near the bog. These species are included as elements in Vorren et al.'s (1990) oligo- and ombrotrophic hummocks and ombro- to mesotrophic lawns, carpets and mudbottom vegetation types.

The relationship between modern vegetation at Hollabåttjønnen Bog and plant wax biomarkers has previously been evaluated (Balascio et al., 2018a). *n*-Alkane compositions vary among vegetation types with a range in average chain lengths from 25-30.5 and a range in hydrogen isotope values of *n*-alkanes from −197‰ to −116‰ among odd-chain length homologs C_{25}-C_{31}. The range of apparent fractionation factors (−66‰ to −134‰) was also established. The average apparent fractionation factor (−108 ± 22‰) is similar to other values reported from the region (Sachse et al., 2006) as well as a global compilation (Sachse et al., 2012). Overall, Balascio et al. (2018a) found significant differences in chain-length distribution patterns and δD values among homologous alkanes in modern vegetation samples, potentially allowing for species-specific interpretations of past changes in δD values. However, they also found that not all vegetation types were equally represented in a surface sediment sample showing that there are complicating factors in how these signals are integrated in the sedimentary record, which we further explore in this study."

Settlement history

Our knowledge of the extent of past human activity at Tønsnes began in 2008, when a series of extensive excavations were conducted by Tromsø University Museum in advance of a planned harbor development. Prior to 2008, only a few limited excavations of site locations from the Stone Age (c. 9500-1800 BC; 11.5-3.8 cal ka BP) and Early Metal Period (c. 1800-0 BC; 3.8-2.0 cal ka BP) had been undertaken in the Tromsø region. In contrast to the limited excavated material, there is an abundance of stray finds and recorded sites extending back to the Early Stone Age in this area. Finds from a c. 18 km section of the coastline from Tønsnes northward to Svarvaren suggest the presence of c. 35 site localities, including 25 from the Late Stone Age (5000-1800 BC; 7.0-3.8 cal ka BP), three from the Iron Age (500 BC – AD 1050; 2.5-0.9 cal ka BP) and five from the Middle Ages and Early Modern Period.

Excavations in 2008-2009 along the southwest margin of the bog documented a number of Mesolithic rectangular house-pit structures of a previously unknown type from the period 7000-6400 BC (9.0-8.4 cal ka BP). These are much larger than is generally the case for Middle Mesolithic house structures in Scandinavia (Skandfer et al., 2010; Gjerde and Skandfer, 2017). Extensive excavations in 2011 and 2012 to the east and north of the bog documented widespread and intensive Stone Age settlement (Gjerde and Hole, 2013). Among the most noteworthy results was the documentation of 40 house structures, principally from the Early Stone Age (9500-5000 BC; 11.5-7.0 cal ka BP), with the earliest dated to c. 9500 cal BC. The structures were situated on shoreline terraces and are circular to oval in appearance with diameters from 2-3 meters. Additional large house-pit structures were also documented. A majority of the excavated house remains were from the period 6300-5400 BC (8.3-7.4 cal ka BP) and were typically small (6-20 m^2), round, oval or rectangular cleared areas with restricted finds. In contrast to the Early Stone Age, which accounted for 87 % of the artifacts recovered, Late Stone Age occupation was restricted to three site locations.

The most recent excavations at Tønsnes took place in 2014 (Nergaard et al., 2016). The focus was on site localities in the southwestern area of the Skarpeneset peninsula extending from the western margin of the bog at c. 25 m a.s.l. westward and downslope to more level locations closer to the ocean at c. 10 m a.s.l. Sites from the Early and Late Stone Age and Early Metal Period were excavated, including house remains, hearths and locations for stone tool production and other activities. The artifact assemblages were varied and included ground slate tools, flaked stone tools and asbestos-tempered ceramics. Excavations revealed extensive use of the area with both summer and winter settlement in addition to more specialized locations over several thousand years. As anticipated by shoreline dating and a steadily dropping sea level during and after the Late Stone Age, a number of sites from the Early Metal Period (1800-0 cal BC; 3.8-2.0 cal ka BP) and to a lesser extent Early Iron Age (AD 0-500; 2.0-1.5 cal ka BP) were revealed at lower elevations including house structures, activity areas, a unique grave cairn and a variety of hearths with and without associated house structures.

Methods

Sediment core collection and bog stratigraphy

A ground-penetrating radar (GPR) survey was conducted, sediment cores were collected from the center of the bog, and peat sections were excavated on the periphery of the bog. GPR profiles were collected with a MALÅ RTA System using a 50 MHz antenna. Data from twenty profiles across the bog were compiled in GPRSoft^{TM}, the base of the peat was identified, and a three-dimensional map of the bog was created. The thickness of the peat was confirmed with sediment cores and excavated sections dug into the bog.

Three peat cores were recovered using a Livingstone square-rod piston corer (TØ-12-A, B, C) and six excavated sections were collected (TØ-13-01–06) (Figure 1) by either digging a shallow pit or extracting a profile from an exposed bog face. Cores and peat sections were split, described, and photographed prior to sampling. Compression of sections occurred during coring as observed by the difference in the recovery length as compared to the length of each drive (1m). All core depths are given accounting for compression. No compression occurred in the excavated sections. We focused the majority of our analysis on core TØ-12-B, 5.16-m long, recovered from the center of the bog surface. Samples were taken to develop the chronology and for pollen and plant wax analysis. In addition, contiguous 5-cm thick samples from core TØ-12-B were taken to analyze the minerogenic content. The samples were dried for 48 hours at 50°C and weighed before and after being ashed at 550°C for 4 hours. The percent minerogenic content was calculated as the weight percent of the ashed sample relative to the initial dried sample.

Chronology

The chronologies of the peat cores and sections are based on radiocarbon dating and tephrochronology. Terrestrial plant macrofossils were picked from sediment surfaces and sent to Direct AMS (Seattle, WA) for radiocarbon analysis. In all, we obtained 30 radiocarbon dates from the Livingstone cores and the six peat profiles (Table 1). All radiocarbon ages were calibrated to calendar years using CALIB v. 7.1 (Stuiver et al., 2017) with the IntCal13 calibration dataset (Reimer et al., 2013). Ages are presented in calendar years prior to AD 1950 unless otherwise indicated. Tephra were also isolated across select sections of core TØ12-B. Tephra in this region are not present as visible layers, but can be found as cryptotephra horizons from distal fallout from, primarily, Icelandic explosive volcanic eruptions and therefore need to be isolated from the peat. Sections 5 cm in thickness from depth intervals: 0-25 cm, 15-65 cm, and 25-75 cm were ashed at 550°C for 4 hours to remove organic material. The remaining ash was washed over a 20-µm sieve then mounted on microscope slides where glass shards were counted using a polarizing light microscope. Samples were prepared for microprobe analysis using a digestion procedure. Samples were treated with H_2O_2 and heated to remove the organic material, then washed over a 20-µm sieve, and mounted on microprobe slides in epoxy resin. Slides were polished to expose grain interiors and analyzed using wavelength dispersive spectrometry on a Cameca SX50 electron microprobe at the University of Massachusetts Amherst, Department of Geosciences using an accelerating voltage of 15 keV, a beam current of 10 nA, and beam size of 5-10 µm. Instrument calibration was performed using a series of silicate minerals, synthetic oxides, and glass standards. Results are reported as non-normalized major oxide concentrations.

Pollen and NPP analyses

For pollen and NPP analysis, 1-cm^3 sediment samples were processed at ~17-cm intervals throughout peat core TØ-12-B. Pollen was processed using a modified Fægri and Iversen (1989) method, with addition of *Lycopodium* tracer tablets, standard chemical treatments and sieving through a Nitex screen for samples with abundant clays or silts. Pollen types were identified using reference samples from the Laboratory of Paleoecology (LOP, Northern Arizona University) as well as pollen keys and reference literature (Moore et al., 1991; Reille, 1992). NPPs were identified based on a number of references commonly used in the LOP, including van Hoeve and Hendrikse (1998), van Geel (2001) and others, the website http://nonpollenpalynomorphs.tsu.ru/ and some of our own publications (Ejarque et al. 2015; Anderson et al. 2015). Because we were interested in a local record, the pollen sum included all gymnosperms and angiosperms noted to occur either on or adjacent to the bog surface. Percentages were determined as a fraction of the pollen sum. NPP and spore percentages were calculated outside the pollen sum. Microfossil percentages were graphed using TILIA, and zoned using the CONISS function software (Grimm, 2005).

Macrofossil analysis

Plant macrofossils were analyzed from five peat sections: TØ-13-01, -02, -03, -04 and -05. Subsamples of 12-15 cc were taken at 1-cm intervals over the length of the profiles. Samples were then soaked in sodium hexametaphosphate and sieved using a 250 µm sieve, and identified and counted under a dissecting microscope. Macrofossil types were identified using the modern LOP reference collection, and several published atlases (Benum, 1958; Montgomery, 1977; Levesque et al., 1988). Concentrations of each identified macrofossil type were standardized to equal volumes and graphed using Tilia software (Grimm, 2005).

Organic and stable isotope geochemistry

Thirty samples from peat core TØ-12-B were collected for lipid biomarker analyses. Lipids were extracted from freeze-dried and homogenized samples with 9:1 (v:v) dichloromethane:methanol using a Dionex Accelerated Solvent Extractor (ASE 350). The total lipid extract (TLE) from all samples was separated using silica gel flash column chromatography. Approximately 0.75 g of pre-cleaned (3x DCM rinsed) and dried activated silica gel (100-200 mesh) was packed in a Pasteur pipette and flushed with 3 bed volumes of hexane (Optima grade, Fisher Scientific). TLE was loaded onto hexane-saturated columns with hexane and eluted with 4 bed volumes each of hexane, dichloromethane, and methanol. The first fraction (hexane eluent) was evaporated and transferred to GC vials, and *n*-alkanes (C_{19}-C_{33}) were identified and quantified on an Agilent 7890A gas chromatograph (GC) equipped with a mass selective detector (MSD) and flame ionization detector (FID). We used a 30-m long Agilent HP-5ms column with inner diameter of 0.25 mm and film thickness of 0.25 um. The GC oven was held for 1.5 min at 60°C, ramped to 150°C at 15°C/minute, then ramped to 320°C at 4°C/minute and held for 10-min. We used a PTV injector in splitless mode, with samples injected at 60°C and the injector temperature immediately ramped to 320°C at 4.5 °C/sec. *n*-Alkane concentrations were converted to fractional abundances of the $C_{19\text{-}33}$ *n*-alkanes to examine the chain-length distributions. 2σ uncertainties of the fractional abundances of the *n*-alkanes $C_{10\text{-}40}$ in a laboratory standard run during the course of the analysis were smaller than 2%. Average chain length (ACL) was determined using the formula:

$$ACL_{19-33} = \frac{\Sigma(C_i\text{-})(X_i)}{\Sigma(C_i)},\ for\ i = 19\text{ - }33$$

where, C_i is µg/g sediment of the *n*-alkane and X_i is the carbon chain-length of each homolog (Poynter et al., 1989). The *Sphagnum*/Vascular Ratio (SVR) was determined using the formula:

$$SVR = -0.0151\left(\frac{C_{23}}{C_{29}}\right)^4 + 0.1144\left(\frac{C_{23}}{C_{29}}\right)^3 - 0.3916\left(\frac{C_{23}}{C_{29}}\right)^2 + 0.8996\left(\frac{C_{23}}{C_{29}}\right) - 0.0455\,,$$

which is a rescaling of the *n*-C_{23} to *n*-C_{29} ratio and represents a comparison of the amount of *Sphagnum*-derived alkanes relative to vascular plant-derived alkanes (Nichols et al., 2006).

δD values of *n*-alkanes (C_{25}-C_{31}) were measured at the Stable Isotope Laboratory at Lamont-Doherty Earth Observatory (LDEO) on a Thermo Delta V isotope ratio mass spectrometer (irMS) coupled to a Thermo Trace GC via a ConFlo IV interface, and using the same column, GC oven program, and injector settings as the GC-MSD/FID analysis. Homologs shorter than C_{25} eluted together with an unresolvable complex mixture and are therefore not reported here. The C_{33} *n*-alkane was not abundant enough for isotope analysis. The hydrogen isotope composition of *n*-alkanes is reported as per mille relative to VSMOW using standard δ notation:

$$\delta D\ (‰) = \left(\frac{R_{sample}}{R_{VSMOW}} - 1\right) \times\ 1000$$

where, R = $^2H/^1H$, the ratio of deuterium to hydrogen, and VSMOW is Vienna Standard Mean Ocean Water. Samples were measured in duplicate, triplicate, or quadruplicate and precision of replicate analyses was typically better than ± 2‰ (1σ). Analytical precision of an external standard measured after every sixth sample injection throughout the course of analysis was better than ± 3‰ (1σ). An authenticated standard lipid mixture with known δD values (A5; Arndt Schimmelmann, Indiana University) was measured regularly during the interval of analysis and was used to determine the apparent δD value of reference H_2 gas, and to convert raw δD measurements to the VSMOW scale (Polissar and D'Andrea, 2014). Uncertainties were determined using the pooled standard deviation approach detailed by Polissar and D'Andrea (2014), which includes the uncertainty of the δD value of the reference H_2 gas on the VSMOW scale as determined from the molecular standards, and the measurement uncertainty of the δD value of each analyte of interest.

Results and discussion

Peat morphology, and stratigraphy

To assess the extent and stratigraphy of the Hollabåttjønnen bog, we analyzed GPR profiles, dug out sections, and collected multiple cores. GPR profiles show a distinct reflector throughout the study site that represents the base of the peat (Figure 2). There are no other reflectors present within the profiles indicating that the bog does not contain any significant minerogenic layers or compositional changes. The basal reflector was mapped on all profiles and used to generate a bog thickness map, which shows that the basal surface generally slopes toward the southwest and the peat is up to 5-6 m thick in the southwestern section (Figure 2). Peat cores and excavated peat sections all extend to the base of the bog, usually ending on gravels or sands, confirming this spatial pattern of bog thickness determined using the GPR (Figure 1 and 2).

Three peat cores (TØ12-A, B, C) were recovered and six peat sections (TØ13-01–06) were excavated (Figure 2). All of the sections generally show an upper light brown peat overlying a darker brown more humified peat, which sits directly on a sandy gravelly surface. Cores TØ12-A and TØ12-C were recovered from the eastern and western sides of the bog (Figure 2), with a total recovery of 5.06 and 3.29 m, respectively (Table 1). In Core A, the upper 1.5 m is fibrous peat with light and dark brown color banding. Below 1.5 m it is generally dark brown to black and from 4.5 – 5.0 m the peat is very dense, indicating a general increase in humification in these intervals. The bottom 0.5 cm contains sand and small gravel. In Core C, the upper 1.5 m is alternating light and dark brown peat. From 1.5-3.1 m the peat is dark brown to black and more humified. The bottom 0.2 m consists of dense sand and gravel.

We focused most of our analyses on core TØ-12-B, which was recovered from the center of the bog with a total recovery of 5.16 m (Figure 2). The upper 2.5 m is fibrous light brown peat with some dark brown horizons. From 2.5 to 4.2 m the peat is dark brown to black and increases in density below 4.2 m. The bottom 30 cm contains some sand and small pebbles in the bottom 1 cm. The minerogenic content of Core B was also assessed and is generally <3% for the majority of the record (Figure 3). There are higher values in the bottom 1 m where values rapidly decrease from 12 to 3%, with the highest values in the bottom 30 cm of the core.

Chronology

Basal ages were obtained for all nine sites (Table 1). The bog sediment thickness map shows that the oldest sections of peat are in the center of the bog where it is the thickest (Table 1; Figure 2). The basal ages of Cores A, B, and C are c. 8.9, 9.4, and 5.4 cal ka BP, respectively (Table 1). Core TØ-12-B was the focus of our detailed paleoenvironmental analysis so additional chronological data was collected to create an age-depth model (Figure 3; Table 1). Nine radiocarbon ages were analyzed from the core, and we also used two tephra horizons that were isolated and identified to define the age-depth relationship.

Tephra were identified as colorless, vesicular grains found throughout the investigated sections with concentrations ranging from 2-853 grains/g of sediment (Figure 3). Tephra grains were small, 20-60 μm in diameter, which made the microprobe analyses difficult and forced us to focus our efforts on the two horizons with the most abundant grains (TØ12-B 230; TØ12-B 358). Samples TØ12-B 230 and TØ12-B 358 contain single geochemical populations of rhyolitic tephra (Table 2; Figure 4) that are similar to tephra erupted from the Hekla volcano, the most active of the central volcanoes in Iceland (Larsen and Eiríksson, 2008).

Tephra in sample TØ12-B 230 are attributed to the Plinian phase of the Hekla 4 eruption dated to c. 4.1-4.5 cal ka BP (reviewed by Zillén et al., 2002). This is a widespread tephra and is found at sites in the British Isles (Dugmore et al., 1995), Sweden (Zillen et al., 2002; Cooper et al., 2019), and in Norway at sites in Lofoten (Pilcher et al., 2005) and Andøya (Vorren et al., 2007) (Table 2). The geochemical data clearly fall within the range of Hekla 4 (Figure 4). However, it should be noted that the standard deviations for some elements are greater than the reference tephra due to the lower analytical totals for these measurements, which occurred because of the small size and vesicular nature of the sample making the microprobe analysis difficult. The age of this tephra is primarily constrained by radiocarbon dating of its occurrence at other North Atlantic sites, but it has also been identified in a varved sequence from Sweden and we use this age (4390 ± 107 cal ka BP) for our age model (Zillén et al., 2002).

The geochemistry of sample TØ-12-B 358 is similar to the Lairg A tephra (c. 6900 cal yr BP) (Table 2; Figure 4). The Lairg A tephra has been found in the British Isles (Dugmore et al., 1995; Pilcher et al. 1996; Chambers et al., 2004), Sweden (Bergman et al., 2004), and in northern Norway at sites in Lofoten (Pilcher et al., 2005) and Andøya (Vorren et al., 2007) (Table 2). The composition of Lairg A does resemble the slightly older Hekla 5 tephra (c. 7300 cal yr BP), however it remains unclear if Lairg A and Hekla 5 represent tephra from two distinct eruptions since separate tephra layers attributed to both eruptions have only been found at two sites (Chamber et al., 2004; Pilcher et al., 2005). We match the TØ-12-B 358 sample to the age of the Lairg A tephra, 6852-6947 cal yr BP, which is based on wiggle-matching of radiocarbon dates at Sluggan Bog (Pilcher et al., 1996).

An age-depth model was created using the radiocarbon ages and tephra in R (R Development Core Team, 2011) using the Clam routine (Blaauw, 2010) (Figure 3). Smooth spline functions, weighted by the probability distributions of the calibrated age ranges, were fitted to the ages to provide an accurate understanding of the age uncertainty of the record. The 95% confidence age ranges are presented and we used the best-fit ages for our chronology (Figure 3). The age model provides information on the rate of peat accumulation over the last 9.4 cal ka BP, which ranged from 0.02-0.17 cm yr^{-1} (Figure 3). From 9.4-7.8 cal ka BP accumulation was relatively constant, 0.06 cm yr^{-1}, and then there was a brief but rapid increase from c. 7.8-6.7 cal ka BP. This was followed by a decrease starting at c. 6.7 cal ka BP, with the lowest rates of peat accumulation from c. 5.4-2.8 cal ka BP. Over the last c. 3 cal ka BP accumulation rates steadily increased in core TØ12-B.

Pollen data

Pollen assemblages were determined from 47 levels in core TØ-12-B. We used the CONISS function of TILIA (Grimm, 2005) to objectively determine pollen zones, using the following 10 types: *Betula*, *Pinus*, *Picea*, *Salix*, *Alnus*, *Betula nana*, *Rubus*, *Empetrum*, Ericaceae and Cyperaceae. CONISS determined five primary zones. Average sampling interval for the 518-cm, 9543-yr core was c. 11 cm and 203 years. The pollen data are graphed in three figures: upland and regional species pollen percentages (Figure 5); bog surface and wetland species pollen percentages (Figure 6); and Non-Pollen Palynomorphs (NPPs) and common ferns (Figure 7).

Pollen Zone 1 (c. 9.5 [bottom of record] – 8.8 cal ka BP): Total pollen concentrations were very low, varying from 1.2k to 10.0k grains/cm^3 (Figure 5). Minor amounts of two pollen types were recovered – *Salix* and *Saxifraga* – along with a few fern spores and VA (vesicular-arbuscular) fungal spores. The lack of pollen and the occurrence of VA fungi (usually found in soils as mycorrhizae) suggest that some of the parent glacial material, or soil that was forming on the glacial deposit, might be mixed into the dry peat. This potentially indicates that there was a short period of time when the site was exposed subaerially, allowing for development of incipient soils.

Pollen Zone 2 (c. 8.8 – 7.7 cal ka BP): Pollen and spore concentrations increase considerably, ranging from 12.8k to 21.4k grains/cc. Dominant pollen types are *Pinus*, with increasing arboreal *Betula*, *Salix*, and *Alnus* with *Betula nana*. Cyperaceae and Poaceae pollen also increase, and fern and *Lycopodium* spores are first found. Pollen of other herbs – Asteraceae, *Potentilla*, *Menyanthes* and Schrophulariaceae – are present. These distributions indicate a period of developing plant diversity and much wetter conditions.

Pollen Zone 3 (c. 7.7 – 3.8 cal ka BP): Generally high pollen concentrations occur in this zone, especially during the later part (to 105.4k grains/cc). *Betula* and *Pinus* pollen percentages decline, as *Alnus,* and especially Ericaceae members (heath shrub family), *Empetrum nigrum* and *Rubus chamaemorus*, expand. *Drosera* pollen is first encountered. Small amounts of *Betula nana* shrub pollen is present. Many herbs are found with the most abundant being Schrophulariaceae and Ranunculaceae (buttercup family). Fern spores are common, especially early in the zone (e.g., *Athyrium*, *Dryopteris* and *Cystopteris*), as are unicellular protists (*Amphitrema flavum*, *Assulina* sp.) and other fungi (*Didymosphaeria*, *Pleospora*). However, towards the end of zone, *Rubus chamaemorus* and peat dwelling unicellular protists (*Amphitrema flavum*, *Assulina* sp.) decline. This period witnessed the development of a heath shrubland, suggesting generally drier conditions.

Pollen Zone 4 (c. 3.8 – 1.0 cal ka BP): Arboreal *Betula* continues to dominate the tree pollen with reduced amounts of *Pinus* and more consistent, but small, amounts of *Picea* (spruce) pollen. Pollen of heath shrubs (Ericaceae, *Empetrum*) decline considerably, replaced by pollen of

Cyperaceae and Poaceae, along with *Rubus chamaemorus* pollen. Ferns are somewhat reduced, but spores of *Sphagnum* reach their maximum c. 2.5-1.5 cal ka BP. These pollen changes define increasingly wetter conditions, especially as the heath shrubs decline. The upland arboreal flora continued to be dominated by *Betula* cf. *pubescens*, but this time with small but consistent amounts of *Picea* pollen showing up in the profile. The latter might indicate decreased temperatures, or may simply be due to delayed immigration of the tree regionally. Spores of *Sordaria*, a coprophilous fungi associated with ungulates (Ejarque et al., 2011) increase late in the zone, associated with pollen of *Rumex* (dock).

Pollen Zone 5 (c. 1.0 cal ka BP– present): After c. 0.96 cal ka BP, arboreal *Betula* pollen generally declines, while pollen of heath shrubs (Ericaceae, *Betula nana*, *Rubus chamaemorus*) increases. Pollen of *Rumex* and *Plantago* increase substantially, later followed by the coprophilous *Sporormiella* and *Sordaria*. This is also a period of fluctuations in unicellular protists, indicative of fluctuating water tables, while pollen of *Rubus chamaemorus* peaks at about 0.4 cal cal ka BP. The resurgence of dwarf shrubs suggests increasingly drier local conditions, or greater development of hummock and hollow bog landforms. The increase in coprophilous fungi is a clear indicator of the presence of ungulates on the bog surface.

Plant macrofossil data

Plant macrofossil assemblages from the excavated peat profiles, TØ-13-01 to -05, demonstrate the evolution of the bog during the late Holocene, and largely parallel the pollen changes documented in Pollen Zones 4 and 5 of core TØ-12-B. Bottom ages of bog profiles TØ-13-01, -02, -03 and -05 suggest lateral growth of the bog by c. 3.3-3.7 cal ka BP, while deposition at TØ-13-04 began somewhat later (~1.6 cal ka BP; Figures S1-S5, Table 1). Each profile originates above bluish gray sand with abundant charcoal, suggestive of local parent material-derived soil that previously periodically burned.

Peat profiles typically are composed of a Poales (Cyperaceae + Poaceae) fragment matrix in the lower portion of the profile, giving way to an upper section where abundant remains of subshrubs were recovered. This transition varies within each profile, as low as >1.9 to ~0.5 cal ka BP (Figures S1-S5). In general, this transition is marked by upcore increases in fruits and leaves of *Betula*, and seeds of *Empetrum nigrum*, Ericaceous shrubs (*Andromeda* cf. *polifolia*, *Vaccinium*) and *Rubus chamaemorus*. Beginning of deposition in most of these profiles generally corresponds to Pollen Zone 4 with greater Cyperaceae and wetter conditions, while the upper transition mostly occurs within or near the beginning of Pollen Zone 5, with increased abundance of subshrubs and drier conditions.

Plant wax distributions and δD values

Sedimentary *n*-alkanes (C_{21}-C_{33}) in the Hollabåttjønnen peat record have a strong odd-over-even predominance, typical for vascular plants (Eglinton and Hamilton, 1967), and show significant changes in distributions over the last 9.5 cal ka BP (Figure 8). From c. 9.5-7.8 cal ka BP, ACL values are ~25, with peaks in concentration of *n*-C_{21}, *n*-C_{23}, and *n*-C_{25}. This interval generally corresponds with Pollen Zones 1 and 2. By c. 7.6 cal ka BP, there is a shift to higher average chain length (ACL) values, ~30, and *n*-C_{29} and *n*-C_{31} are the dominant homologs. However, concentrations of mid-chain alkanes are elevated from c. 7.6 to 5.0 cal ka BP, and ACL values gradually increase through this interval until c. 3.5 cal ka BP, the end of Pollen Zone 3 (Figure 8). At c. 3.5 cal ka BP, there is a slight shift to lower ACL values, but n-C_{29} and n-C_{31} are still the most abundant and display only minor variations corresponding to Pollen Zones 4 and 5.

Another indicator of distribution changes is the *Sphagnum*/Vascular Ratio (SVR). In the Hollabåttjønnen record SVR is highly correlated with ACL (R=0.986) and possibly indicates that the greatest relative proportions of *Sphagnum* existed from c. 9.5-7.8 cal ka BP, were lower from 7.8-3.5 cal ka BP, and were slightly higher but variable from 3.5 cal ka BP to present (Figure 8). However, Balascio et al. (2018a) found that a *Sphagnum* sample from this site did not contain significant amounts of n-C_{23} through n-C_{25} and that other plants did have relatively high amounts of mid-chain length n-alkanes. Moreover, the identification of a distinct peak in *Sphagnum* spores c. 2.5-1.5 cal ka BP does not correspond to a significant increase in mid-chain length n-alkanes (Figure 7, 8), all of which confounds the interpretation of SVR ratios at this site.

n-Alkane δD values of n-C_{25}, n-C_{27}, n-C_{29}, n-C_{31}, and n-C_{33} range from −229‰ to −158‰ (Figure 8). Values are similar among mid-chain (n-C_{25}, n-C_{27}) and long-chain (n-C_{29}, n-C_{31}, n-C_{33}) length n-alkanes, respectively. δD values of mid-chain length n-alkanes covary with long-chain length homologs for parts of the record, but are generally more depleted. To represent the relative differences between mid-chain and long-chain compounds we also plot the δD of n-C_{33}-C_{25} (Figure 9C). We compare the difference in δD values between n-C_{33} and n-C_{25} because we consider the longest homolog the least likely to be produced by a wide variety of vegetation, and therefore the most likely to represent a constant apparent fractionation from environmental water throughout the record. From 9.5-7.8 cal ka BP, corresponding to Pollen Zones 1 and 2, δD values all of the chain-lengths covary and have similar average values. After 7.8 cal ka BP, the δD values of mid-chain length compounds decrease and generally remain more depleted throughout the rest of the record (with the exception of the sample at 5.0 cal ka BP). The largest difference in δD values between mid- and long-chain compounds (up to 40‰) occurred from c. 7.3 to 2.6 cal ka BP. The long-chain length compounds also exhibit a slight increasing trend of ~20‰, from c. 7.3 to 2.5 cal ka BP. After 2.5 cal ka BP, there is a decline in the δD values of long-chain compounds and they become more similar to δD values of mid-chain length homologs. Interestingly, the large difference in δD values between mid- and long-chain compounds corresponds approximately with the start of Pollen Zone 3 (Figure 8). δD values among mid- and long-chain length compounds become more similar at c. 1.1 cal ka BP, corresponding to the transition from Pollen Zone 4 to 5, but mid-chain compounds again are more depleted over the last c. 0.5 cal ka BP.

Paleoenvironmental implications

The morphology of the Hollabåttjønnen Bog, its stratigraphy, and chronology provide information on the Holocene climate evolution of this region. The Skarpeneset peninsula, on which the Hollabåttjønnen Bog formed, is a Lateglacial recessional moraine of the Balsfjord glacier deposited during the Skarpnes event c. 14.5-14.0 cal ka BP when relative sea level was ~65-70 m above modern (Andersen, 1968; Vorren and Plassen, 2002). The basal date from the deepest section of the bog (TØ-12-B) shows that the onset of peat growth, at a present elevation of 20 m a.s.l., occurred c. 9.4 cal ka BP (Table 1). There is no evidence for any transitional sediment that would indicate that a pond or marine embayment existed prior to peat growth. Thus, the claim by Gjerde and Skandfer (2017) that this central bog area was a natural, sheltered harbor cannot be supported by our data. A sea-level elevation of 20 m at c. 9.4 cal ka BP corresponds with sea level data from Lyngen, ~35 km east of our site, which shows that following ice retreat relative sea level dropped from ~70 m to ~20 m by c. 9.4 cal ka BP (Corner and Haugane, 1993; Bakke et al., 2005). The timing of sea level lowering below 20 m in Lyngen is similar to the timing of the onset of formation of the Hollabåttjønnen bog indicating that the bog likely started to grow immediately after the site rebounded. A mid-Holocene sea-level transgression, Tapes transgression, also impacted this region c. 6.5 cal ka BP. A beach ridge associated with the Tapes is evident on the northwest and northeast side of Skarpeneset with a Tapes maximum documented at 16 m a.s.l. (Gjerde and Hole, 2013), but it is below the base of the peat deposit and did not affect sedimentation in Hollabåttjønnen Bog. Following the onset of peat formation we define three primary Holocene paleoenvironmental intervals based on pollen, macrofossil, and plant wax data:

Early Holocene (c. 9.5-7.7 cal ka BP)

Following the establishment of the bog, c. 9.5 cal ka BP, pollen data indicate increasingly wetter conditions than at the base of the profile during the early Holocene with our record showing increased organic matter, higher total pollen concentration, and plant richness until 7.7 cal ka BP (Figure 9). Dominant pollen types are *Pinus*, with increasing arboreal *Betula*, *Salix*, and *Alnus* with *Betula nana*. *Cyperaceae* and *Poaceae* pollen also increase, and fern and *Lycopodium* spores are first identified. It is likely that *Betula pubescens* grew near the site, but pollen percentages suggest that *Pinus* cf. *sylvestris* was either rare or distantly placed, perhaps on adjacent uplands near the site. Willows and dwarf birch were also at the site, but the bog vegetation consisted primarily of wetland sedges and grasses.

Plant wax distributions also suggest wet early Holocene conditions with this interval marked by higher concentrations of mid-chain length *n*-alkanes and relatively low ACL values (Figure 8, 9C). *n*-Alkane δD values are variable during this interval, which is evidence for a high degree of variability in temperature and/or moisture source changes. However, most striking is that this is the only time when all of the homologs have similar values likely reflecting little evaporation and similarities in source water for all homologs, which we interpret to reflect increased surface wetness and higher water table conditions (Figure 9C).

These trends in vegetation during the early Holocene are similar to those documented east of our site in Finnmark (Huntley et al., 2013) and reflect regional warming conditions in response to insolation driven climate changes (Seppä et al., 2009; Sejrup et al., 2016) (Figure 9). Wet conditions accompanying regional warming have also been documented in northern Fennoscandia by pollen data from further south in northern Norway until c. 7.9 cal ka BP (Bjune and Birks, 2008), and by higher lake levels in northern Finland until c. 8.0 cal ka BP (Eronen et al., 1999).

Mid-Holocene (c. 7.7-3.8 cal ka BP)

During the mid-Holocene, pollen data indicate distinctly drier conditions (Figure 9). We show that the site was a heath shrubland with increasing concentrations of Ericaceae, *Empetrum nigrum* and *Rubus chamaemorus*, and various species of ferns from 7.8-3.8 cal ka BP. Wetland Poales (primarily sedges and grasses) were at a minimum. Dry conditions are also supported by a decrease in the bog accumulation rate, which is the lowest during the latter part of this interval, c. 5.4-3.0 cal ka BP (Figure 3).

Plant wax distributions also show distinctly different conditions starting around this time. They show an abrupt shift to higher ACL values c. 7.8 cal ka BP, as well as the onset of significant differences between δD values of mid- and long-chain length *n*-alkanes from c. 7.8-2.5 cal ka BP, aside from the sample at c. 5.1 cal ka BP (Figure 9C). The isotopic offset between long and mid-chain alkanes could indicate that this period marks the onset of contributions from different plant sources that may access water that has undergone varying degrees of evaporation. For example, *n*-alkanes can derive from plants without a vascular system, which use water near the surface of the bog subject to greater evaporation, and from plants with vascular systems, which access water from deeper in the bog where relative evaporation rates might be lower. Our pollen data show that there was a shift in vegetation documented as a decrease in herbaceous plants and increase in subshrub plants c. 7.7 cal ka BP at the start of this interval, which we interpret to indicate drier conditions (Figure 9). Modern vegetation shows a range of values among homologous *n*-alkanes of the same plant type, but there is not a clear relationship between the δD values between mid- and long-chain length *n*-alkanes and plants with and without vascular systems (Figure 9; Balascio et al., 2018a). We also cannot rule out that *n*-alkanes may come from vegetation sources on the landscape surrounding the bog, which further complicates this relationship. Regardless, trends in δD values of long-chain length waxes (e.g. n-C_{29}), typically attributed to vascular plants that are less impacted by evaporation, show only minor variations across this interval aside from a gradual rise in values. This trend suggests that changes in precipitation isotopes may have been relatively minor.

Paleoclimate records from northern Fennoscandia generally show maximum temperatures and drier conditions during this interval associated with the regional timing of the Holocene Thermal Maximum (HTM). Vegetation and climate reconstructions from northern Norway show the warmest Holocene conditions c. 8.5-4.3 cal ka BP in Finnmark (Huntley et al., 2013), and c. 8.0-3.5 cal ka BP around Mo i Rana (Bjune and Birks, 2008). There is evidence for lower lake levels in northern Finland from 8.0-4.0 cal ka BP (Eronen et al., 1999), and pollen-based temperature reconstructions from northern Europe define the warmest period from 8.0-4.8 cal ka BP (Seppä et al., 2009). Nearby proglacial lake records that receive runoff from the Langfjordjøkelen Ice Cap and Lenangsbreene also shows that ice was absent or very restricted from until c. 4.1 cal ka BP, and c. 3.8 cal ka BP, respectively (Bakke et al., 2005; Wittmeier, et al., 2015) (Figure 9B). More broadly, climate records synthesized from throughout the North Atlantic-Fennoscandian region show a similar timing of changes and maximum Holocene temperatures, which are interpreted to reflect a delayed response to Northern Hemisphere summer insolation (Sejurp et al., 2016) (Figure 9A).

Late Holocene (c. 3.8 cal ka BP - present)

The onset of late Holocene conditions began c. 3.8 cal ka BP with a shift in vegetation suggesting increasingly wetter conditions, and as a result a more extensive development of the hummock and hollow form characteristic of the bog surface today. In general, pollen of heath shrubs (Ericaceae, *Empetrum*) declined considerably, while pollen of wetland Poales (particularly Cyperaceae) increased, along with *Rubus chamaemorus* pollen. The general anti-phase percentages (Figure 6) during this period between Poales and *Rubus* is consistent with the hummock and hollow bog form, with wetter hollows supporting the Poales and somewhat drier *Rubus* and, less generally, other Ericaceae growing on hummocks. TØ-12-B shows an increase in accumulation rate across this interval (Figure 3), basal ages from peat sections collected around the periphery of the bog provide evidence for lateral expansion of the bog after c. 3.5 cal ka BP (Table 1; Figure 2), and peat petrology of excavated profiles show they are composed of a matrix of Poales species, which also supports wetter conditions (Figures S1-S5). These conditions are concurrent with the increase in coprophilous fungi, c. 1 cal ka BP, indicating the presence of ungulates and likely increasing human impact on the bog.

Plant wax data show a slight decrease in ACL and increase in mid-chain length δD values c. 3.8 cal ka BP, but changes in long chain-length δD values lag the vegetation changes and exhibit a shift to lower values after c. 2.5 cal ka BP (Figure 9). This lagged response may indicate that long-chain length δD values reflect a change in precipitation isotopes rather than a change in plant type. The decline in δD values of precipitation isotopes after 2.5 cal ka BP may be a response to colder temperatures or less Atlantic-sourced precipitation. Interestingly, the marked decline in long-chain length δD values right at 2.5 cal ka BP corresponds to the peak in *Sphagnum* spores. Balascio et al. (2018a) found that *Sphagnum* and an unidentified moss sample had among the most negative δD values of the modern plants sampled, likely explaining this relationship. Overall, the last 2.5 cal ka BP also shows a slight decrease in the difference between δD values of mid- and long-chain length *n*-alkanes, although there is greater variability in this relationship. This potentially reflects vegetation changes between the mid- to late Holocene in response to the wetter conditions indicated by pollen data and/or changes in the proportion of *n*-alkanes derived from plants accessing water that has undergone varying degrees of evaporation.

The late Holocene in northern Norway is generally defined by cooler and wetter conditions. Colder growing season conditions and southward retreat of treeline has been found in Finnmark over the last 4.3 cal ka BP (Huntley et al., 2013), and starting c. 3.5 cal ka BP further south near Mo i Rana (Bjune and Birks, 2008). This interval also corresponds with a rise in lake water levels in Finland, c. 4.0 cal ka BP (Eronen et al., 1999), the rejuvenation of the Langfjordjøkelen Ice Cap, c. 4.1 cal ka BP, and Lenangsbreene, c. 3.8 cal ka BP in northern Norway (Bakke et al., 2005; Wittmeier et al., 2015), and the overall decline of temperatures in the North Atlantic-Fennoscandian region (Sejrup et al., 2016) (Figure 9).

Paleoenvironmental perspective on human-environment interactions during the Holocene at Hollabåttjønnen Bog

There are intriguing correlations between settlement phases at Tønsnes and the Holocene climate and environment intervals identified using pollen macrofossils, and plant wax biomarkers. The earliest dates for settlement around 9.5 cal ka BP (Gjerde and Hole, 2013; Gjerde and Skandfer,

2017) roughly coincide with establishment of the bog. The early Holocene represents pioneer settlement and the earliest house structures were small, circular to oval tent-like constructions occupied during the summer along the shoreline (Gjerde and Skandfer, 2017). The appearance of large pit-house structures at the transition from the early to middle Holocene c. 8.0 cal ka BP coincides with the onset of drier conditions influencing available bog-related resources. This is also the most intensive settlement phase with 26 house structures in addition to middens and activity areas. There is considerable variation in house size and form although a majority are interpreted as lightly constructed lean-to or tent structures used during the summer season. Evidence of Late Stone Age and Early Metal Period occupation was minimal prior to the 2014 excavations when a cluster of sites from these periods was documented below the western rim of the bog (Nergaard et al., 2016). This coincides with increasingly wetter conditions and expansion of the bog during the late Holocene that may have restricted available habitation locations to lower elevations between the ocean and the bog margins.

Settlement evidence following the Early Metal Period is limited to several hearth features dated to the period AD 0-500 during the Early Iron Age (Nergaard et al., 2016). Although the possibility of additional Iron Age or later settlement sites on the peninsula outside of the excavated areas cannot be ruled out, it is considered unlikely based on lack of evidence following intensive archaeological survey and testing in the area. The appearance of *Sordaria* coprophilous fungal spores late in pollen zone 4 indicates that ungulates were present on the bog surface during the Late Iron Age. The continued presence of grazing animals in the vicinity over the past c. 500 years is documented by *Sporormiella* and *Sordaria* fungal spores in pollen zone 5. Given the lack of evidence for agricultural settlement in the Tønsnes area during the Viking Age (AD 800-1050), Middle Ages (AD 1050-1550) and early modern period, it is most likely that the ungulates in question were reindeer rather than domesticated livestock. Wild reindeer are unlikely to have been present in close proximity to prehistoric settlement sites at Tønsnes and the sudden appearance of coprophilous fungi at c. 1 cal ka BP suggests more concentrated reindeer-related activity than would be the case with the occasional presence of wild reindeer. Tønsnes is a historic reindeer gathering location associated with annual migrations between the coast and inland that continues to be used by the indigenous Sámi today. Recent high-resolution palynological analyses of paired peat profiles at a recently abandoned reindeer gathering pen near Jokkmokk in northern Sweden have demonstrated the impact of reindeer herding through coprophilous fungal spores (Kamerling et al., 2017). Evidence for a much weaker fungal spore signal from the core furthest from the pen area is consistent with the typically shorter dispersal distances for these microfossils. The situation at Tønsnes may be analogous with a weak spore signal from the core at the center of the bog compared with cores from the bog margin, a hypothesis that can only be tested through further analyses.

Proxy indicators for reindeer husbandry have been recorded at a number of locations in the region. These include the appearance of coprophilous (*Sporomiella*) fungal spores in mire sediment cores from Dividalen in northern Troms in the 17th century that can be confidently linked to reindeer grazing by Sámi pastoralists (Sjögren and Kirchhefer, 2012). Sámi reindeer pastoralism in nearby Devddesvuopmi as early as the 15th century has been inferred on the basis of archaeological evidence (Sommerseth, 2011). The appearance of *Sporomiella* spores at c. AD 1100 in bog sediment profiles from an historical reindeer gathering site in Lavangsdalen, a straight-line distance of c. 34 km southeast of Tønsnes, is also interpreted as representing reindeer herding activity (Sjögren, 2013). Sámi reindeer management involved the exploitation of multiple resources with a gradual transition from hunting to pastoralism and potential domestication in the Viking Age (Storli, 1993; Bergman et al., 2013; Bjørklund, 2013).

Conclusions

Holocene climate and environmental changes reconstructed from Hollabåttjønnen Bog provide improved perspectives on past climate trends in northern Norway and environmental conditions relevant to the history of local human activity. Based on analysis of pollen, plant macrofossils, and plant wax biomarkers we show the sensitivity of this peat bog to hydroclimate changes and evidence for direct human impacts. In particular, we define three distinct climate intervals, including the early Holocene (c. 9.5-7.7 cal ka BP) when wetter conditions are defined by the presence of wetland sedges and grasses, higher concentrations of mid-chain length *n*-alkanes, and a similarity in δD values among the homologs. During the mid-Holocene (c. 7.7-3.8 cal ka BP), we infer drier conditions based on heath shrubland vegetation, low peat accumulations rates, and significant differences between δD values of mid- and long-chain length *n*-alkanes. Wetter conditions are associated with the late Holocene (c. 3.8 cal ka BP-present), marked by lateral bog expansion, and an increase in sedges and grasses. Our analysis of *n*-alkane chain-length distribution patterns and δD values shows significant trends over the Holocene related to vegetation and hydroclimate changes. In comparison with results from modern vegetation data, they also highlight some limitations in leaf wax δD interpretations of the Holocene evolution of this wetland setting.

Evidence for human activities near and on the bog come from both archaeological excavations on the periphery of the bog, and from the sediment cores. The oldest documented settlements at c. 9.5 cal ka BP are nearly contemporaneous with the origination of the incipient bog. Subsequent structures dating to the Late Stone Age to Early Iron Age suggest continued settlement within the bog vicinity for much of the Holocene. Sediments deposited over the last c.1 cal ka BP also record likely evidence of human impact on the bog itself, marked by vegetation change and the presence of coprophilous fungi potentially associated with reindeer grazing activity. Conclusions from our multiproxy study, combined with the available archaeological evidence, provides evidence that fits clearly within the progression of human activities in the region.

Acknowledgements

This research was supported by funding to NLB, RSA, and SW from the Port of Tromsø, in conjunction with cultural heritage mitigation for the Grøtsund port facility. The Vetlesen Foundation and the Center for Climate and Life at LDEO also provided financial support that helped make the study possible. We would like to thank Michael Kelly, A. Jeltsch-Thömmes, Jeremiah Nickerson, Silke Buschmann and Sophia Delzell for assistance in the laboratory, and two anonymous reviewers for comments on an earlier draft of this manuscript.

References

Aaby B (1976) Cyclic climatic variations in climate over the last 5,500 years reflected in raised bogs. *Nature* 263: 281-284.

Amesbury MJ, Barber KE and Hughes, PDM (2012) The relationship of fine-resolution, multi-proxy palaeoclimate records to meteorological data at Fågelmossen, Värmland, Sweden and the implications for the debate on climate drivers of the peat-based record. *Quaternary International* 268: 77-86.

Andersen BG (1968) Glacial geology of Western Troms, North Norway. *Norges Geologiske Undersøkelse* 256: 1-160.

Anderson, RS, Ejarque, A, Rice, J, Smith, S, Lebow, C. 2015. Historic and Holocene Environmental Change in the San Antonio Creek Basin, Mid-coastal California. *Quaternary Research* 83, 273-286.

Balbo AL, Persson P and Roberts SJ (2010) Changes in settlement patters on the River Rena, southeast Norway: A response to Holocene climate change? *The Holocene* 20: 917-929.

Baas M, Pancost RD, van Geel, B et al. (2000) A comparative study of lipids in *Sphagnum* species. *Organic Geochemistry* 31: 535-541.

Bakke J, Dahl SO, Paasche Ø et al. (2005) Glacier fluctuations, equilibrium-line altitudes and palaeoclimate in Lyngen, northern Norway, during the Lateglacial and Holocene. *The Holocene* 15: 518-540.

Bakke J, Lie Ø, Dahl SO et al. (2008) Strength and spatial patterns of the Holocene wintertime westerlies in the NE Atlantic region. *Global and Planetary Change* 60: 28-41.

Balascio NL and Anderson RS (2014) Paleoenvironmental analysis of Hollabåttjønnen Bog, Skarpeneset Peninsula, Tønsnes, Norway. Final Report. Appendix 3 in: Nergaard, R.H., Oppvang, J. and Cerbing, M., 2016. Tønsnes Havn, Tromsø kommune, Troms. Rapport fra de arkeologiske undersøkelsene 2014. *Tromura kulturhistorie nr. 45*, Tromsø: Tromsø Museum, University of Tromsø, 191-214.

Balascio NL and Wickler S (2018) Human-environment dynamics during the Iron Age in the Lofoten Islands, Norway. *Norsk Geografisk Tidsskrift* 72: 146-160.

Balascio NL, D'Andrea WJ, Anderson RS et al. (2018a) Influence of vegetation type on *n*-alkane composition and hydrogen isotope values from a high latitude ombrotrophic bog. *Organic Geochemistry* 121: 48-57.

Balascio NL, D'Andrea WJ, Gjerde M, Bakke J (2018b) Hydroclimate variability of High Arctic Svalbard during the Holocene inferred from hydrogen isotopes of leaf waxes. *Quaternary Science Reviews* 183: 177-187.

Barber KE (1993) Peatlands as scientific archives of past biodiversity. *Biodiversity and Conservation* 2: 474–489.

Barber KE, Chambers FM, Maddy D et al. (1994) A sensitive high-resolution record of late Holocene climatic change from a raised bog in northern England. *The Holocene* 4: 198–205.

Barber KE (2006) Peatland records of Holocene climate change. In: Elias, S. (Ed.) Encyclopedia of Quaternary Science. Elsevier, Oxford, p. 1884-1895.

Battarbee RW and Binney HA (2008) Natural climate variability and global warming: a Holocene perspective. Wiley-Blackwell Publishing Ltd, pp. 276.

Benum P (1958) The Flora of Troms Fylke. Tromsø Museums Skrifter, Volume VI. Tromsø Museum, Tromsø, Norway.

Bergman J, Wastegård S, Hammarlund D et al. (2004) Holocene tephra horizons at Klocka Bog, west-central Sweden: aspects of reproducibility in subarctic peat deposits. *Journal of Quaternary Science* 19: 241-249.

Bergman I, Zackrisson O, Liedgren L (2013) From hunting to herding: land use, ecosystem processes, and social transformation among Sami AD 800-1500. *Arctic Anthropology* 50 (2): 25-39.

Bjerck HB (2008) Norwegian mesolithic trends. In Bailey, G. and Spikins, P. Eds., *Mesolithic Europe*. Cambridge University Press, 60-106.

Bjune AE and Birks HJB (2009) Holocene vegetation dynamics and inferred climate changes at Svanåvatnet, Mo I Rana, northern Norway. *Boreas* 37: 146-156.

Bjørklund I (2013) Domestication, reindeer husbandry and development of Sámi pastoralism. *Acta Borealia* 30(2): 174-189.

Bowen GJ and Revenaugh J (2003) Interpolating the isotopic composition of modern meteoric precipitation. *Water Resources Res*earch 39: 1299.

Blaauw M (2010) Methods and code for 'classical' age-modelling of radiocarbon sequences. *Quaternary Geochronology* 5: 512-518.

Blackford JJ and Chambers FM (1991) Proxy records of climate from blanket peat: evidence for a Dark Age (1400 BP) climatic deterioration in the British Isles. *The Holocene* 1: 63-67.

Blackford JJ and Chambers FM (1993) Determining the degree of peat decomposition for peat based palaeoclimatic studies. *International Peat Journal* 5: 7–24.

Breivik HM (2014) Palaeo-oceanographic development and human adaptive strategies in the Pleistocene-Holocene transition: A study from the Norwegian coast. *The Holocene* 24: 1478-1490.

Bush RT and McInerney FA (2013) Leaf wax *n*-alkane distributions in and across modern plants: implications for paleoecology and chemotaxonomy. *Geochimica et Cosmochimica Acta* 117: 161-179.

Calvo E, Grimalt J and Jansen E (2002) High resolution Uk37 sea surface temperature reconstruction in the Norwegian Sea during the Holocene. *Quaternary Science Reviews* 21: 1385-1394.

Chambers FM, Barber KE, Maddy D et al. (1997) A 5500-year proxy-climate and vegetation record from blanket mire at Talla Moss, borders, Scotland. *The Holocene* 7: 391–399.

Chambers FM, Daniell JRG, Hunt JB et al. (2004) Tephrostratigraphy of An Loch Mór, Inis Oírr, western Ireland: implications for Holocene tephrochronology in the northeastern Atlantic region. *The Holocene* 14: 703-720.

Charman DJ (1999) Testate amoebae and the fossil record: issues in biodiversity. *Journal of Biogeography* 26: 89-96.

Charman DJ, Barber KE, Blaauw M et al. (2009) Climate drivers for peatland paleoclimate records. *Quaternary Science Reviews* 28: 1811-1819.

Cooper CL, Swindles GT, Watson EJ et al. (2019) Evaluating tephrochronology in the permafrost peatlands of northern Sweden. *Quaternary Geochronology* 50: 16-28.

Corner GD and Haugane E (1993) Marine-lacustrine stratigraphy of raised coastal basins and postglacial sea-level change at Lyngen and Vanna, Troms, northern Norway. *Norsk Geologisk Tidsskrift* 77: 175-197.

Curtin L, D'Andrea WJ, Balascio NL, Pugsley G, de Wet G, Bradley R (2019) Holocene and Last Interglacial climate of the Faroe Islands from sedimentary plant wax hydrogen and carbon isotopes. *Quaternary Science Reviews* 223: 105930.

Diefendorf AF, Freeman KH, Wing SL et al. (2011) Production of *n*-alkyl lipids in living plants and implications for the geologic past. *Geochimica et Cosmochimica Acta* 75: 7472-7485.

Diefendorf AF, Leslie AB and Wing SL (2015) Leaf wax composition and carbon isotopes vary among major conifer groups. *Geochimica et Cosmochimica Acta* 170: 145-156.

Dugmore AJ, Larsen G and Newton AJ (1995) Seven tephra isochrones in Scotland. *The Holocene* 5: 257–266.

Eglinton G and Hamilton RJ (1967) Leaf epicuticular waxes. *Science* 156: 1322-1335.

Ejarque, A, Anderson, RS, Simms, AR, Gentry, BJ. 2015. Prehistoric fires and the shaping of colonial transported landscapes in southern California: a palaeoenvironmental study at Dune Pond, Santa Barbara County. *Quaternary Science Reviews* 112, 181-196.

Ejarque A, Miras Y and Riera S (2011) Pollen and non-pollen palynomorph indicators of vegetation and highland grazing activities obtained from modern surface and dung datasets in the eastern Pyrenees. *Review of Palaeobotany and Palynology* 167: 123-139.

Eldevik T, Risebrobakken B, Bjune AE et al. (2014) A brief history of climate – the northern seas from the Last Glacial Maximum to global warming. *Quaternary Science Reviews* 106: 225-246.

Eronen M, Hyvärinen H and Zetterberg P (1999) Holocene humidity changes in northern Finnish Lapland inferred from lake sediments and submerged Scots pines dates by tree-rings. *The Holocene* 9: 569-580.

Fægri K and Iversen J (1989) Textbook of Pollen Analysis (4th edn by Faegri, K., Kaland, P.E, Krzywinski, K.). New York, NY: Wiley.

Gjerde JM and Hole J-T (2013) Tønsnes Havn, Tromsø kommune, Troms. Rapport frå dei arkeologiske undersøkingane 2011 og 2012. *Tromura kulturhistorie nr. 44*, Tromsø: Tromsø Museum, University of Tromsø.

Gjerde JM and Skandfer M (2017) Large Mesolithic house-pits at Tønsnes, coastal northern Norway: evidence of a winter aggregation site? In: *Early Economy and Settlement in Northern Europe. Pioneering, Resource Use, Coping with Change*, The Early Settlement of Northern Europe, Volume 3. Ed. Blankholm, H.P. Sheffield: Equinox Publishing, 59-76.

Glørstad H (2014) Deglaciation, sea level changes and the Holocene colonisation of Norway. In Harff, J., Bailey, G., Lüth, F. (eds.), *Geology and Archaeology; Submerged Landscapes of the Continental Shelf.* Special Publication of the Geological Society of London. 9-26.

Grimm EC (2005) TILIA and TILIA GRAPH. PC spreadsheet and graphics software for pollen data. Illinois State Museum, Springfield, IL.

Hald M, Andersson C, Ebbesen H et al. (2007) Variations in temperature and extent of Atlantic Water in the northern North Atlantic during the Holocene. *Quaternary Science Reviews* 26: 3423-3440.

Huntley B, Long AJ and Allen JRM (2013) Spatio-temporal patterns in Lateglacial and Holocene vegetation and climate of Finnmark, northernmost Europe. *Quaternary Science Reviews* 70: 158-175.

Jansen E, Andersson C, Moros M et al. (2008) The early to mid Holocene thermal optimum in the northern North Atlantic and Nordic Seas: the role of seasonal orbital forcing and Holocene century to millennial scale climate events. In Battarbee, R.W. and Binney, H.A., editors, Natural climate variability and global warming: a Holocene per- spective. Blackwell Publishing Ltd, 123–37.

Kahmen A, Schefuß E and Sachse D (2013a) Leaf water deuterium enrichment shapes leaf wax *n*-alkane δD values of angiosperm plants I: experimental evidence and mechanistic insights. *Geochimica et Cosmochimica Acta* 111: 39-49.

Kahmen A, Hoffmann B, Schefuß E et al. (2013b) Leaf water deuterium enrichment shapes leaf wax *n*-alkane δD values of angiosperm plants II: observational evidence and global implications. *Geochimica et Cosmochimica Acta* 111: 50-63.

Kamerling IM, Schofield JE, Edwards KJ and Aronsson K-Å (2017) High-resolution palynology reveals the land use history of a Sami *renvall* in northern Sweden. *Vegetation History and Archaeobotany* 26: 369-388.

Larsen G and Eiríksson J (2008) Late Quaternary terrestrial tephrochronology of Iceland – frequency of explosive eruptions, type and volume of tephra deposits. *Journal of Quaternary Science* 23: 109-120

Levesque PEM, Dinel H and Larouche A (1988) Guide to the Identification of Plant Macrofossils in Canadian Peatlands. Agricultural Canada, Research Branch, Publication 1817. Land Resource Research Centre, Ottawa, Canada.

Möller P, Östlund O, Barnekow L et al. (2012) Living at the margin of the retreating Fennoscandian Ice Sheet: The early Mesolithic sites at Aareavaara, northernmost Sweden. *The Holocene* 23: 104-116.

Montgomery FH (1977) Seeds and Fruits of Plants of Eastern Canada and Northeastern United States. University of Toronto Press, Toronto.

Moore PD, Webb JA and Collison ME (1991) Pollen Analysis. Blackwell Scientific, London.

Mossberg B and Stenberg L (2010) Gyldendals Nordiske Feltflora. Gyldendal Norsk Forlag.

Nergaard RH, Oppvang J and Cerbing M (2016) Tønsnes Havn, Tromsø kommune, Troms. Rapport fra de arkeologiske undersøkelsene 2014. *Tromura kulturhistorie nr. 45*. Tromsø: Tromsø Museum, University of Tromsø.

Nesje A, Jansen E, Birks JB et al. (2005) Holocene climate variability in the North Atlantic region: a review of marine and terrestrial evidence. In: Drange, H., Dokken, T., Furevik, T., Gerdes, R., Berger, W.H. (Eds.) The Nordic Seas: an integrated perspective , AGU Geophysical Monograph, 289-322.

Nesje A, Bakke J, Dahl SO et al. (2008) Norwegian mountain glaciers in the past, present and future. *Global and Planetary Change* 60: 10-27.

Nichols JE, Booth RK, Jackson ST et al. (2006) Palohydrologic reconstruction based on *n*-alkane distributions in ombrotrophic peat. *Organic Geochemistry* 37: 1505–1513.

Nichols JE, Walcott M, Bradley RS et al. (2009) Quantitative assessment of precipitation seasonality and summer surface wetness using ombrotrophic sediments from an Arctic Norwegian peatland. *Quaternary Research* 72: 443-451.

Nichols JE, Booth RK, Jackson ST, Pendall EG, Huang Y (2010) Differential hydrogen isotopic ratios of *Sphagnum* and vascular plant biomarkers in ombrotrophic peatlands as a quantitative proxy for precipitation—evaporation balance. *Geochimica et Cosmochimica Acta* 74: 1407-1416.

Nicholas, J.E., Peteet, D.M., Moy, C.M., Castañeda, I.S., McGeachy, A., Perez, M., 2014. Impacts of climate and vegetation change on carbon accumulation in a south-central Alaskan peatland assessed with novel organic geochemical techniques. *The Holocene* 24: 1146-1155.

Nott CJ, Xie S, Avsejs LA et al. (2000) *n*-Alkane distributions in ombrotrophic mires as indicators of vegetation change related to climactic variation. *Organic Geochemistry* 31: 231-235.

Oldfield F (2008) The role of people in the Holocene. In Battarbee, R.W. and Binney, H.A., Eds, *Natural climate variability and global warming: a Holocene perspective.* Wiley-Blackwell Publishing Ltd., 58-97.

Pancost RD, Baas M, van Geel B et al. (2002) Biomarkers as proxies for plant inputs to peats: an example from a sub-boreal ombrotrophic bog. *Organic Geochemistry* 33: 675-690.

Pilcher JR, Hall VA and McCormac FG (1996) An outline tephrochronology for the Holocene of the north of Ireland. *Journal of Quaternary Science* 11: 485-494.

Pilcher J, Bradley RS, Francus P et al. (2005) A Holocene tephra record from the Lofoten Islands, Arctic Norway. *Boreas* 34: 136-156.

Polissar PJ and D'Andrea WJ (2014) Uncertainty in paleohydrologic reconstructions from molecular δD values. *Geochimica et Cosmochimica Acta* 129: 146-156.

Poynter J, Farrimond P, Robinson N et al. (1989) Aeolian-derived higher plant lipids in the marine sedimentary record: links with palaeoclimate. In: Paleoclimatology and Paleometeorology: Modern and Past Patterns of Global Atmospheric Transport, Eds. Leinen, M., Sarnthein, M., Springer, Netherlands, 435-462.

R Development Core Team (2011) R: A Language and Environment for Statistical Computing. Vienna: R Foundation for Statistical Computing, available from: www.R-project.org.

Reille M (1992) Pollen et spores d'Europe et d'Afrique du nord. Laboratoire de Botanique historique et Palynologie, Universite d'Aix-Marseille, Marseille, France

Reimer PJ, Bard E, Bayliss A et al. (2013) IntCal13 and Marine13 radiocarbon age calibration curves 0–50,000 years cal BP. *Radiocarbon* 55: 1869-1887.

Risebrobakken B, Jansen E, Andersson C et al. (2003) A high-resolution study of Holocene paleoclimatic and paleoceanographic changes in the Nordic Seas. *Palaeoceanography* 18: 1017.

Risebrobakken B, Moros M, Ivanova EV et al. (2010) Climate and oceanographic variability in the SW Barents Sea during the Holocene. *The Holocene* 20: 609-621.

Rowley-Conwy P and Piper S (2016) Hunter-Gatherer variability: developing models for the northern coasts. *Arctic* 69: 1-14.

Sachse D, Radke J and Gleixner G (2006) δD values of individual *n*-alkanes from terrestrial plants along a climatic gradient – implications for the sedimentary biomarker record. *Organic Geochemistry* 37: 469–483.

Sachse D, Billault I, Bowen GJ et al. (2012) Molecular paleohydrology: interpreting the hydrogen-isotopic composition of lipid biomarkers from photosynthesizing organisms. *Annual Review of Earth and Planetary Sciences* 40: 221–249.

Sejrup HP, Seppä H, McKay NP et al. (2016) North Atlantic-Fennoscandian Holocene climate trends and mechanisms. *Quaternary Science Reviews* 147: 365-378.

Seppä H, Bjune AE, Telford RJ et al. (2009) Last nine-thousand years of temperature variability in northern Europe. *Climate of the Past* 5: 523-535.

Sjögren P (2013) Paleoekolgiska undersökingar i samband med utvidgelse av E8 i Lavangsdalen. Rapport fra naturvitenskapelig undersøkelser. Tromsø: Tromsø Museum, University of Tromsø.

Sjögren P and Kirchhefer AJ (2012) Historical legacy of the old-growth pine forest in Dividalen, northern Scandes. *International Journal of Biodiversity Science, Ecosystem Services and Management* 8(4): 338-350.

Skandfer M, Grydeland SE, Henriksen S (2010) Tønsnes havn, Tromsø kommune, Troms. Rapport fra arkeologiske utgravinger i 2008 og 2009. *Tromura kulturhistorie 40*. Tromsø: Tromsø Museum, University of Tromsø.

Sommerseth I (2011) Archaeology and the debate on the transition from reindeer hunting to pastoralism. *Rangifer* 31(1):111-127.

Storli I (1993) Sámi Viking Age pastoralism – or the "fur trade" reconsidered. *Norwegian Archaeological Review* 26(1): 1-20.

Stuiver M, Reimer PJ, and Reimer RW (2017) CALIB 7.1 [WWW program] at http://calib.org

van Geel, B. 2001. Non-pollen palynomorphs. IN Smol, JP, et al., (Eds.), Tracking Environmental Change Using Lake Sediments, vol. 3. Kluwer Academic Publishers, Dordrecht, pp. 99-119. doi: 10.1007/0-306-47668-1.

van Hoeve, ML, Hendrikse, M. (Eds). 1998. A study of non-pollen objects in pollen slides; the Types as described by Dr Bas van Geel and colleagues. Private printing, Utrecht, The Netherlands

Vorren K-D, Nilssen E and Mørkved B (1990) Age and agricultural history of the '-staðir' farms of North and Central Norway. *Norsk Geografisk Tidsskrift* 44: 79-102.

Vorren K-D, Eurola S, Tveraabak U (1999) The lowland terrestrial mire vegetation about 69 N lat. In northern Norway. Universitetet I Tromsø, Tromsø Museum, Tromsø.

Vorren K-D, Blaauw M, Wastegård S et al. (2007) High-resolution stratigraphy of the northernmost concentric raised bog in Europe: Sellevollmyra, Andøya, northern Norway. *Boreas* 36: 253-277.

Vorren K-D, Jensen CE and Nilssen E (2012) Climate changes during the last c. 7500 years as recorded by the degree of peat humification in the Lofoten region, Norway. *Boreas* 41: 13-30.

Vorren TO and Plassen L (2001) Deglaciation and paleoclimate of the Andfjor-Vågsfjord area, North Norway. *Boreas* 31: 97-125.

Warner BG and Charman DJ (1994) Holocene changes on a peatland in northwestern Ontario interpreted from testate amoebae (Protozoa) analysis. *Boreas* 23: 270–279.

Wittmeier HE, Bakke J, Vasskog K et al. (2015) Reconstructing Holocene glacier activity at Langfjordjøkelen, Arctic Norway, using multi-proxy fingerprinting of distal glacier-fed lake sediments. *Quaternary Science Reviews* 114: 78-99.

Woodland W, Charman DJ and Sims PC (1998) Quantitative estimates of water tables and soil moisture in Holocene peatlands from testate amoebae. *The Holocene* 8: 261-273.

Zillén LM, Wastegård S and Snowball IF (2002) Calendar year ages of three mid-Holocene tephra layers identified in varved lake sediments in west central Sweden. *Quaternary Science Reviews* 21: 1583-1591.

Tables

Table 1. Radiocarbon results for peat cores and peat sections from the Holobåttjønnen Bog (calibrated with CALIB 6.0 using the INTCAL09 dataset). Asterisks next to ages indicate result is out of stratigraphic order.

Table 2. Major oxide concentrations of tephra shards isolated from core TØ12-B compared to reference tephra.

Figures

Figure 1. Location of Hollabåttjønnen Bog in northern Norway (A.) north of the island of Tromsø (B), and showing the location of peat sections and cores with their basal radiocarbon ages in calendar years before present (ka) (Table 1) (C.).

Figure 2. Aerial photograph of Hollabåttjønnen Bog showing a shaded image of the bog thickness determined by ground-penetrating radar (GPR), and core locations. GPR profile from a select transect, A to A’, showing the strong basal reflector indicating the transition from peat to the underlying dense gravelly material.

Figure 3. (Left) Age-depth model (black curve) for core TØ12-B showing radiocarbon and tephra ages. The intervals searched for cryptotephra are shaded in gray with tephra counts indicated and showing distinct peaks where tephra matched the Icelandic volcanic eruptions of Hekla 4 and Hekla 5 or Lairg A. (Center) Accumulation rate based on the age model. (Right) Minerogenic content of core TØ12-B.

Figure 4. Comparison of the geochemical composition of tephra isolated from core TØ12-B and tephra attributed to Hekla 4, Lairg A, and Hekla 5. Geochemical data shown in Table 2.

Figure 5. Upland and regional pollen percentages, as well as total pollen concentrations, from Hollabåttjønnen Bog core TØ 12-B, graphed against depth and age. Pollen zones determined using the CONISS subroutine in TILIA (Grimm, 2005). Silhouette is 10x actual value.

Figure 6. Bog and wetland plant pollen and spore percentages from Hollabåttjønnen Bog core TØ 12-B, graphed against depth and age. Pollen zones determined using the CONISS subroutine in TILIA (Grimm, 2005). Silhouette is 10x actual value.

Figure 7. NPP (non-pollen palynomorph) and common fern spore percentages from Hollabåttjønnen Bog core TØ 12-B, graphed against depth and age. Percentages determined outside the pollen sum. Pollen zones determined using the CONISS subroutine in TILIA (Grimm, 2005). Silhouette is 10x actual value.

Figure 8. *n*-Alkane data for samples from core TØ12-B, including the relative abundance of long-chain length compounds (A.) and mid-chain length compounds (B.), average chain length (ACL) and *Sphagnum*-Vascular Ratio (SVR) (C.), and hydrogen isotope values for mid- and long-chain length compounds (D.).

Figure 9. Trends in North Atlantic-Fennoscandian temperatures (Sejrup et al., 2016) (A.) and Ti data from Lake Jøkelvatnet that were used to reconstruct activity of the Langfjordjøkelen Ice Cap in northern Norway (Wittmeier et al., 2015) (B.) compared with plant wax data (C.) and pollen data (D.-F.) from Hollabåttjønnen Bog. The average difference between δD values of n-C_{33} and C_{25} shown as horizontal dashed line (C.).

Figure S1. Plant macrofossil and charcoal (>250 µm) concentrations from Hollabåttjønnen Bog recalculated to #'s/100 cc in sediments from peat profile TØ 13-01. Vegetative macrofossils shown in green; propagules in orange. Poales vegetation fragments include both Poaceae and Cyperaceae. Median ages (cal ka BP) rounded to one decimal point. Ages in red with asterisk were rejected as being too old (5.8 cal ka BP) or too young (2.7 cal ka BP).

Figure S2. Plant macrofossil and charcoal (>250 µm) concentrations from Hollabåttjønnen Bog recalculated to #'s/100 cc in sediments of peat profile TØ 13-02. Vegetative macrofossils shown in green; propagules in orange. Poales vegetation fragments include both Poaceae and Cyperaceae. Median ages (cal ka BP) rounded to one decimal point. Age in red with asterisk was rejected as being too young.

Figure S3. Plant macrofossil and charcoal (>250 µm) concentrations from Hollabåttjønnen Bog recalculated to #'s/100 cc in sediments of peat profile TØ 13-03. Vegetative macrofossils shown in green; propagules in orange. Poales vegetation fragments include both Poaceae and Cyperaceae. Median ages (cal ka BP) rounded to one decimal point.

Figure S4. Plant macrofossil and charcoal (>250 µm) concentrations from Hollabåttjønnen Bog recalculated to #'s/100 cc in sediments of peat profile TØ 13-04. Vegetative macrofossils shown in green; propagules in orange. Poales vegetation fragments include both Poaceae and Cyperaceae. Median ages (cal ka BP) rounded to one decimal point.

Figure S5. Plant macrofossil and charcoal (>250 µm) concentrations from Hollabåttjønnen Bog recalculated to #'s/100 cc in sediments of peat profile TØ 13-05. Vegetative macrofossils shown in green; propagules in orange. Poales vegetation fragments include both Poaceae and Cyperaceae. Median ages (cal ka BP) rounded to one decimal point; age in red with asterisk was rejected as being too young.

Table 1. Radiocarbon results for peat cores and peat sections from the Holobåttjønnen Bog (calibrated with CALIB 7.10 using the INTCAL13 dataset). Asterisks next to ages indicate the result is out of stratigraphic order.

Core/Section	Depth (cm)	Elevation (m a.s.l)	Description	Laboratory #	$\delta^{13}C$ ‰	^{14}C Age (yr BP)	Calibrated Age Range (yr BP) (1 σ)	(2 σ)	Median Age (cal yr BP)
Peat Cores									
TØ-12-A	156	23.4	Plant/wood fragments	D-AMS 001465	--	2448 ± 40	2377-2694	2358-2705	2525
TØ-12-A	456	20.4	Plant/wood fragments	D-AMS 001461	-23.1	8015 ± 37	8783-9004	8729-9012	8885
TØ-12-B	47	24.5	Plant/wood fragments	D-AMS 006416	-28.1	550 ± 25	531-622	521-633	552
TØ-12-B	0	25.0	Plant/wood fragments	D-AMS 001984	-27.2	1027 ± 30	927-959	832-1048	945
TØ-12-B	122	23.8	Plant/wood fragments	D-AMS 006417	-23.7	1309 ± 25	1187-1287	1183-1292	1257
TØ-12-B	200	23.0	Plant/wood fragments	D-AMS 001463	-27.9	3175 ± 25	3373-3443	3362-3448	3401
TØ-12-B	262	22.4	Plant/wood fragments	D-AMS 006418	-29.7	4959 ± 30	5651-5721	5609-5740	5684
TØ-12-B	200	23.0	Plant/wood fragments	D-AMS 001985	-22.4	5313 ± 33	6008-6179	5992-6192	6089
TØ-12-B	300	22.0	Plant/wood fragments	D-AMS 001464	-16.5	6322 ± 30	7178-7278	7173-7309	7254
TØ-12-B	400	21.0	Plant/wood fragments	D-AMS 001986	-32.4	7626 ± 37	8387-8435	8373-8518	8417
TØ-12-B	502	20.0	Plant/wood fragments	D-AMS 001987	--	8376 ± 46	9317-9470	9285-9490	9408
TØ-12-C	305	23.0	Plant/wood fragments	D-AMS 001460	-23.6	4652 ± 32	5318-5449	5312-5467	5405
Peat Sections									
TØ-13-01	60.5	26.4	Wood, arthropod chitin	D-AMS 006097	-21.8	1973 ± 24	1891-1946	1877-1987	1922
TØ-13-01	104.5	26.0	Arthropod chitin	D-AMS 006098	-25.0	2253 ± 50	2161-2340	2152-2348	2238
TØ-13-01	127	25.7	Plant/wood fragments	D-AMS 003962	-29	5023 ± 31*	5668-5885	5660-5892	5790*
TØ-13-01	127	25.7	Plant/wood fragments	D-AMS 003961	-22.6	2560 ± 29	2621-2749	2504-2753	2724
TØ-13-01	126.5	25.7	Wood, seed	D-AMS 006099	-24.0	3128 ± 27	3271-3383	3251-3440	3355
TØ-13-02	15.5	25.3	Wood fragments	D-AMS 006100	-27.8	323 ± 24	314-433	307-463	387
TØ-13-02	15.5	25.3	Carbon spherules	D-AMS 006101	-26.1	393 ± 21	343-501	333-507	478
TØ-13-02	37	25.1	Charcoal	D-AMS 006102	-20.6	3033 ± 25	3181-3323	3163-3340	3234
TØ-13-02	38.5	25.1	Plant/wood fragments	D-AMS 005166	-25.4	166 ± 21*	7-279	0-285	186*
TØ-13-03	17.5	25.8	Wood fragments	D-AMS 006103	-35.7	1525 ± 25	1368-1515	1349-1521	1407
TØ-13-03	36	25.6	Plant/wood fragments	D-AMS 005167	-31.1	3442 ± 27	3641-3812	3617-3827	3697
TØ-13-04	18.5	26.8	Wood fragments	D-AMS 006104	-27.0	423 ± 23	486-509	342-518	498
TØ-13-04	29	26.7	Plant/wood fragments	D-AMS 005168	-32.1	1720 ± 22	1570-1692	1563-1698	1625
TØ-13-05	39.5	23.6	Wood fragments	D-AMS 006105	-27.9	1243 ± 23	1174-1260	1082-1265	1211
TØ-13-05	39	23.6	Plant/wood fragments	D-AMS 005171	-26.8	1266 ± 28	1181-1261	1091-1284	1223
TØ-13-05	48	23.5	Plant/wood fragments	D-AMS 005169	-25.5	3078 ± 27	3247-3347	3217-3362	3291
TØ-13-05	48	23.5	Plant/wood fragments	D-AMS 005170	-24.2	122 ± 32*	22-266	10-273	122*
TØ-13-06	91	24.1	Plant/wood fragments	D-AMS 004318	-29.1	3135 ± 24	3277-3386	3255-3441	3364

Table 2. Major oxide concentrations of tephra shards isolated from core TØ12-B compared to reference tephras.

Sample	n	SiO_2	TiO_2	Al_2O_3	MgO	CaO	MnO	FeO	Na_2O	K_2O	Cl	Total
TØ-12-B 230 cm	12	71.98 (1.34)	0.12 (0.07)	13.04 (0.80)	0.04 (0.06)	1.21 (0.28)	0.05 (0.03)	1.88 (0.09)	3.45 (0.37)	2.64 (0.12)	0.08 (0.03)	94.51 (1.64)
Hekla 4 - Reference (1,5)	13	72.62 (1.17)	0.12 (0.04)	13.14 (0.43)	0.05 (0.09)	1.38 (0.20)	--	2.03 (0.53)	4.07 (0.40)	2.85 (0.28)	--	96.28 (1.28)
TØ-12-B 358 cm	21	74.63 (1.41)	0.08 (0.01)	12.77 (0.24)	0.04 (0.03)	1.25 (0.06)	0.04 (0.03)	1.66 (0.10)	3.72 (0.33)	2.67 (0.13)	0.05 (0.01)	96.94 (1.67)
Lairg A - Reference (2,3,4)	75	73.18 (1.36)	0.14 (0.12)	12.67 (0.39)	0.05 (0.11)	1.35 (0.29)	0.08 (0.04)	1.86 (0.64)	4.10 (0.38)	2.83 (0.33)	--	96.21 (0.94)
Hekla 5 - Reference (1)	21	74.65 (0.90)	0.13 (0.02)	12.79 (0.19)	0.05 (0.02)	1.29 (0.05)	--	1.71 (0.05)	4.13 (0.14)	2.79 (0.06)	--	97.53 (1.16)

References: 1. Pilcher et al. (2005) 2. Dugmore et al. (1995) 3. Pilcher et al. (1996) 4. Hall and Pilcher (2002) 5. Vorren et al. (2007)

Figure 1.

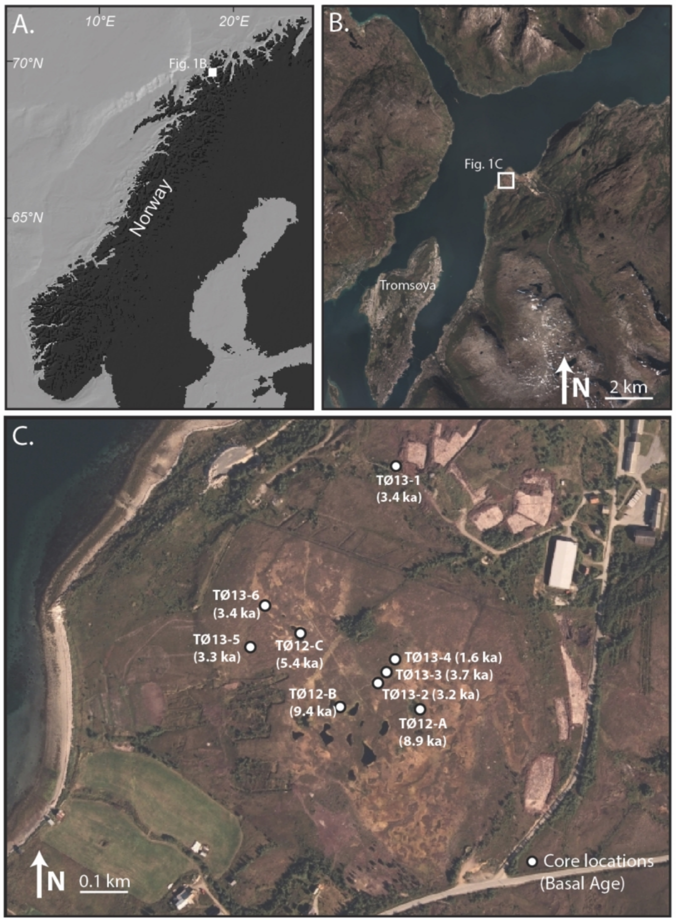

Figure 1. Location of Hollabåttjønnen Bog in northern Norway (A.) north of the island of Tromsø (B), and showing the location of peat sections and cores with their basal radiocarbon ages in calendar years before present (ka) (Table 1) (C.).

508x508mm (300 x 300 DPI)

Figure 2.

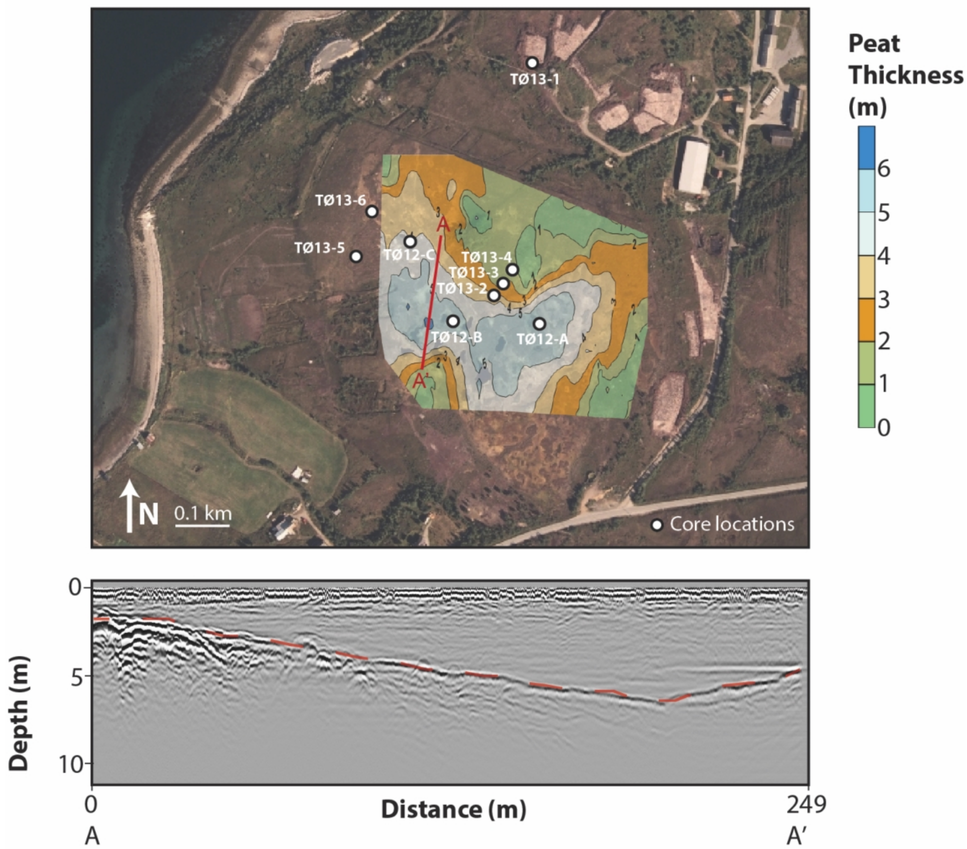

Figure 2. Aerial photograph of Hollabåttjønnen Bog showing a shaded image of the bog thickness determined by ground-penetrating radar (GPR), and core locations. GPR profile from a select transect, A to A', showing the strong basal reflector indicating the transition from peat to the underlying dense gravelly material.

508x526mm (300 x 300 DPI)

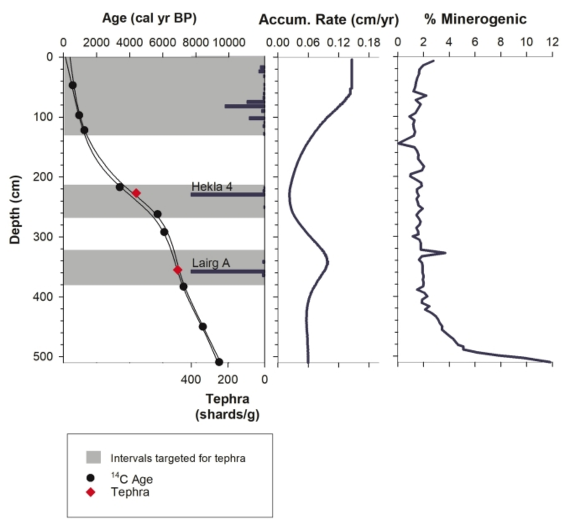

Figure 3. (Left) Age-depth model (black curve) for core TØ12-B showing radiocarbon and tephra ages. The intervals where we searched for cryptotephra are shaded in gray with tephra counts indicated and showing distinct peaks where tephra matched the Icelandic volcanic eruptions of Hekla 4 and Hekla 5 or Lairg A. (Center) Accumulation rate based on the age model. (Right) Minerogenic content of core TØ12-B.

508x392mm (300 x 300 DPI)

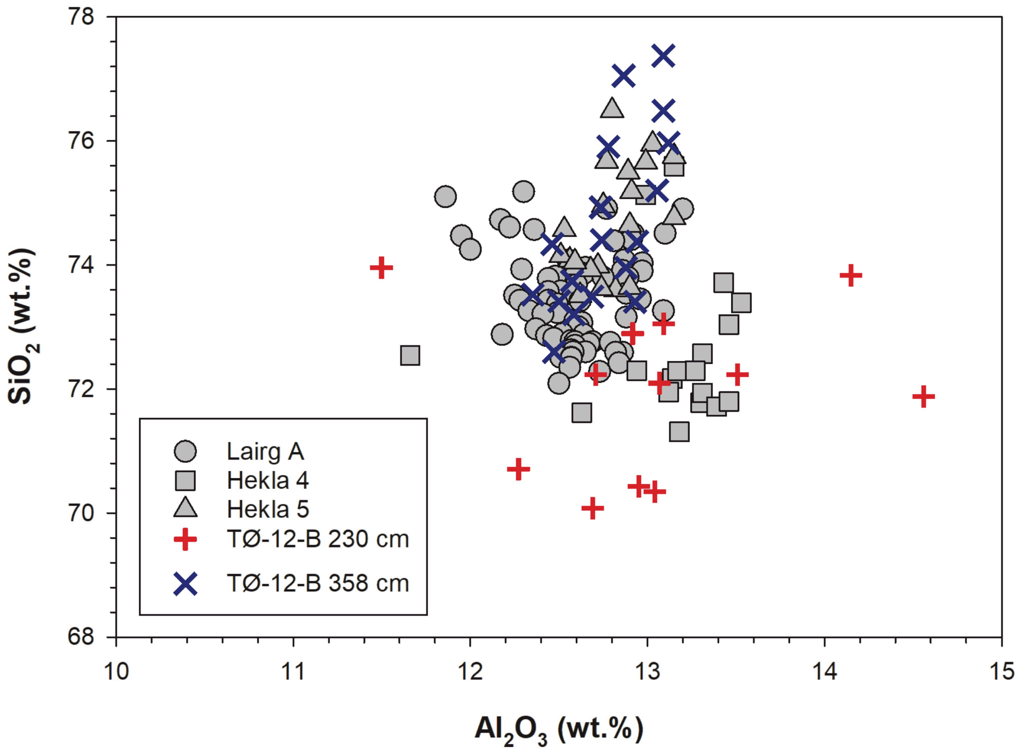
78
76
74
72
70
68
SiO$_2$ (wt.%)
10
11
12
13
14
15
Al$_2$O$_3$ (wt.%)
Lairg A
Hekla 4
Hekla 5
TØ-12-B 230 cm
TØ-12-B 358 cm

Hollabåttjønnen Bog, Troms, Norway (TØ-12-B) Upland & Regional pollen %

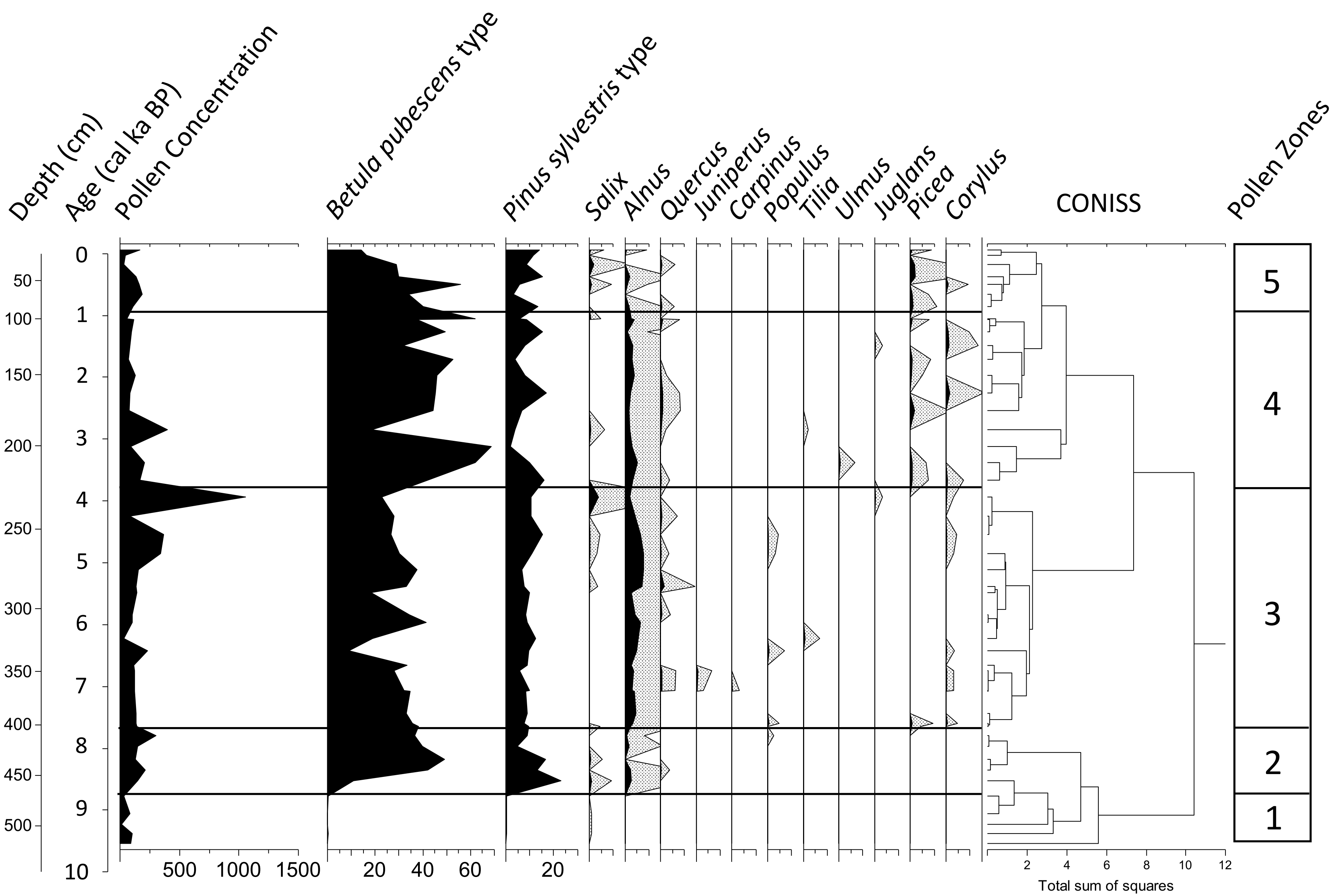

Hollabåttjønnen Bog, Troms, Norway (TØ-12-B) Bog and Wetland pollen & spore %

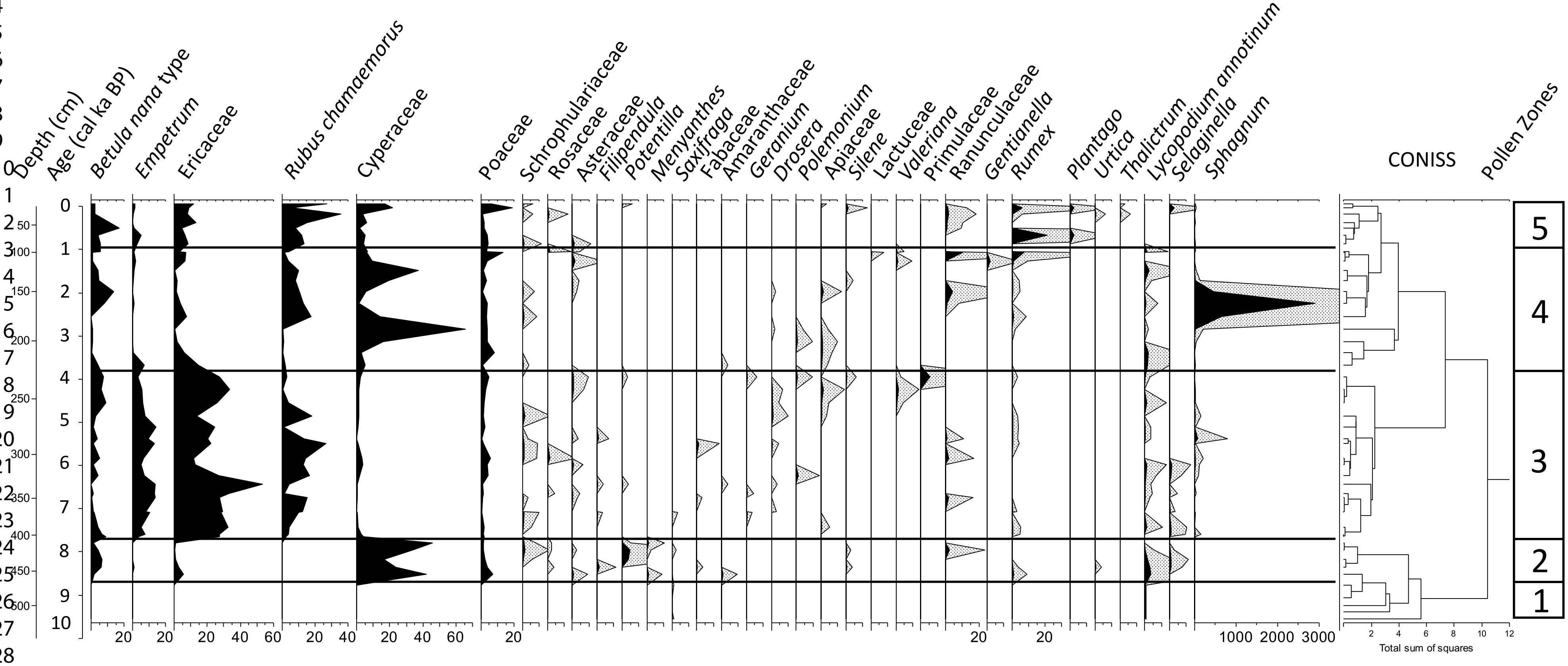

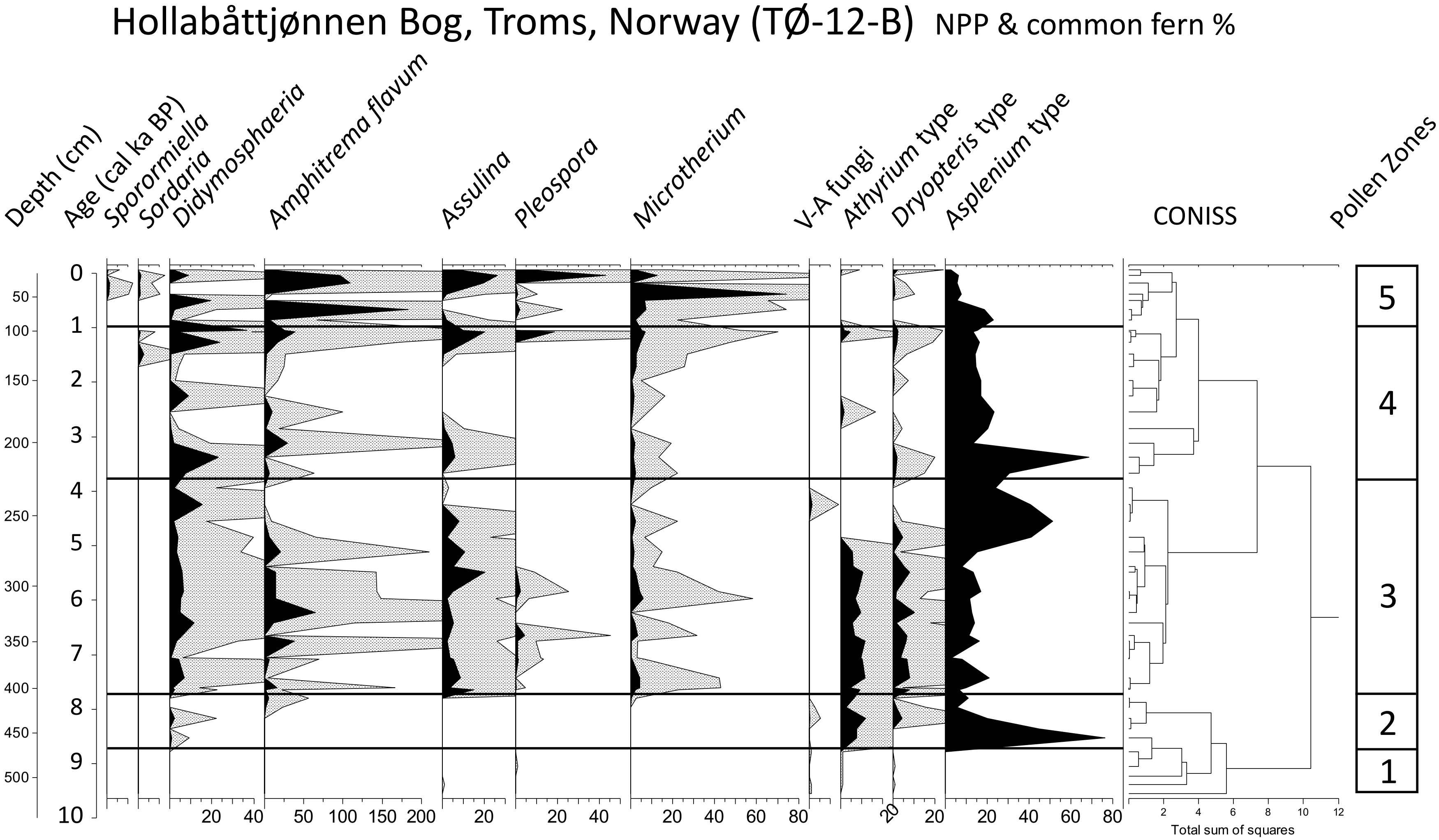
Hollabåttjønnen Bog, Troms, Norway (TØ-12-B) NPP & common fern %
Depth (cm)
Age (cal ka BP)
Sporormiella
Sordaria
Didymosphaeria
Amphitrema flavum
Assulina
Pleospora
Microtherium
V-A fungi
Athyrium type
Dryopteris type
Asplenium type
CONISS
Pollen Zones
Total sum of squares
5
4
3
2
1

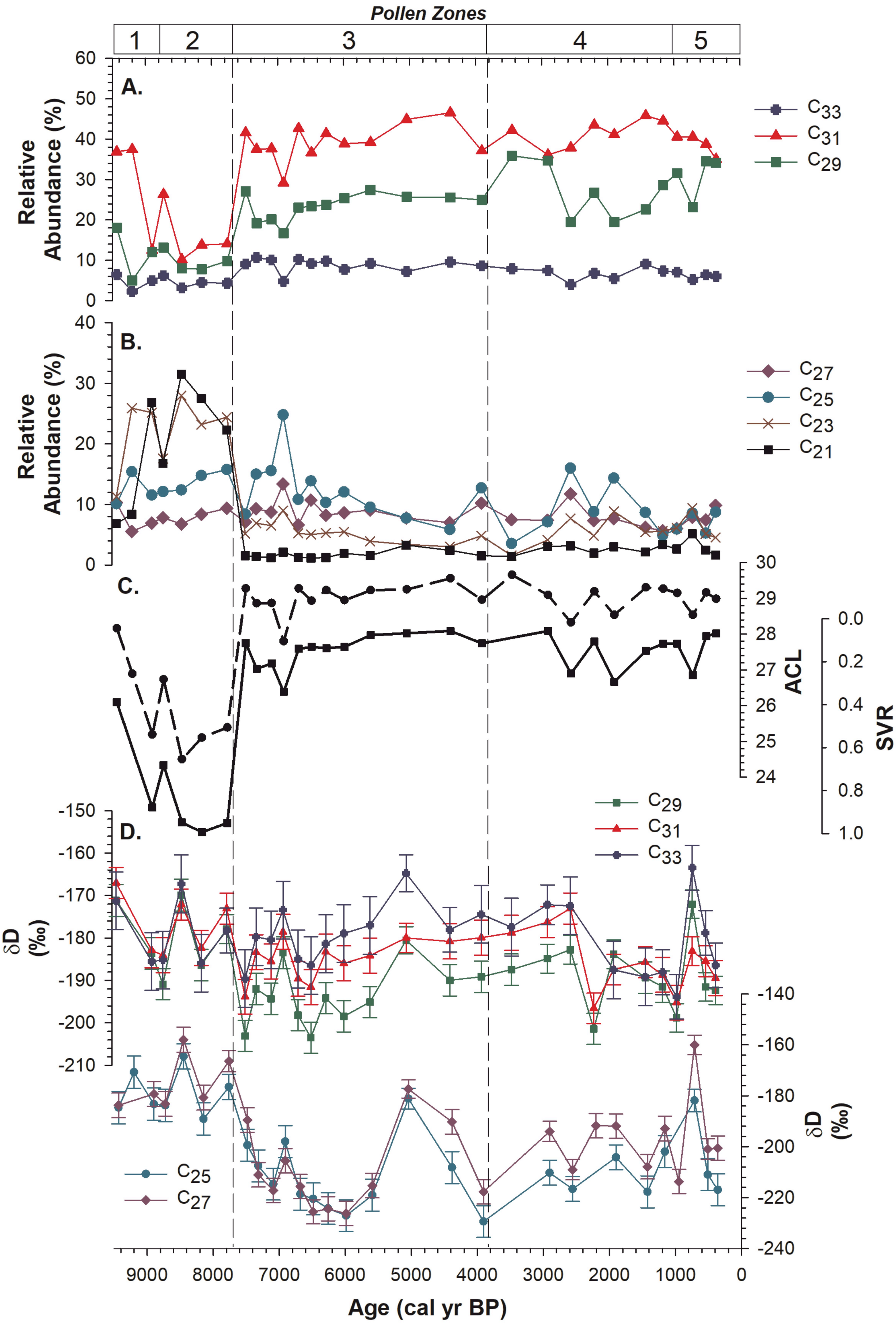
Pollen Zones
1
2
3
4
5
A.
Relative Abundance (%)
C33
C31
C29
B.
Relative Abundance (%)
C27
C25
C23
C21
C.
ACL
SVR
D.
δD (‰)
C29
C31
C33
C25
C27
δD (‰)
Age (cal yr BP)

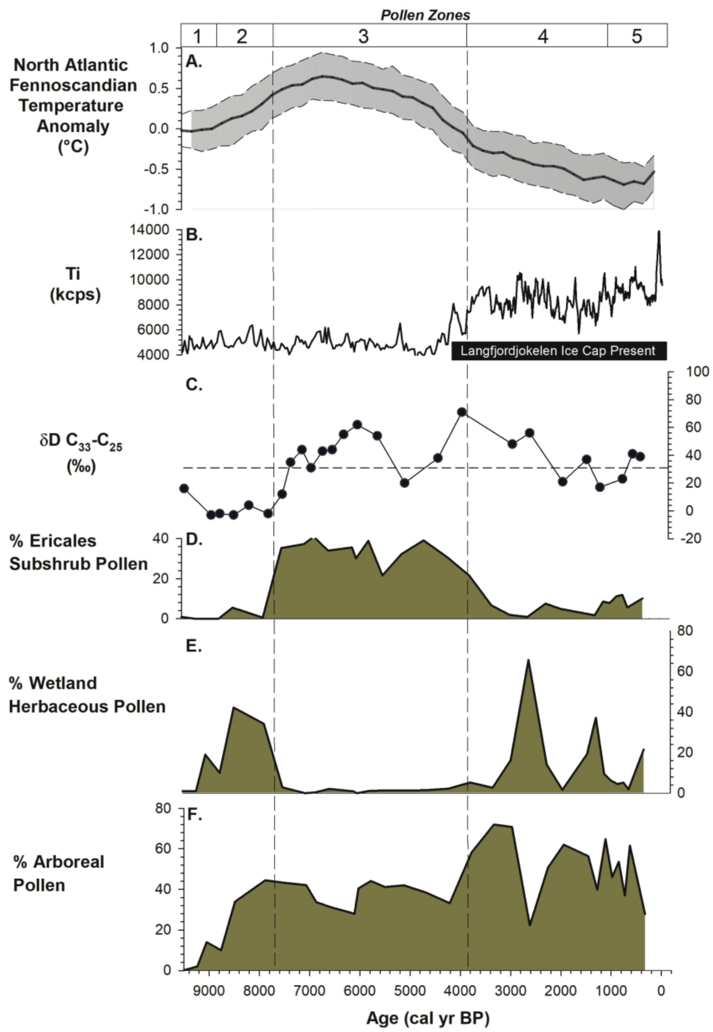

Trends in North Atlantic-Fennoscandian temperatures (Sejrup et al., 2016) (A.) and Ti data from Lake Jøkelvatnet that were used to reconstruct activity of the Langfjordjøkelen Ice Cap in northern Norway (Wittmeier et al., 2015) (B.) compared with plant wax data (C.) and pollen data (D.-F.) from Hollabåttjønnen Bog. The average difference between δD values of n-C33 and C25 shown as horizontal dashed line (C.).

423x547mm (300 x 300 DPI)

Supplemental Information

Peat sections

Plant macrofossil assemblages and charcoal concentrations were assessed for the excavated peat profiles TØ-13-01 to TØ-13-05 collected from around the edges of the bog (Figures 1, S1-S5; Table 1). In addition, detailed stratigraphic information was recorded. TØ13-01 was excavated from the far northeastern portion of the bog; profiles TØ13-02, -03 and -04 were taken from the southwest flank of the central upland; and TØ13-05 came from the west side of the bog (Figure 1).

TØ13-01 consists of 148 cm of peat, with medium brown peat above 125 cm, transitioning through a potential recurrence surface to dark brown peat to 141 cm. Between 141 and 148 cm is a dark brown sandy peat that sits on top of gray sand and light gravels, and consisted of 148 cm of peat. Basal dates vary from ~2.7 and ~3.4 cal ka BP to ~5.8 cal ka BP (Table 1).

TØ13-02 is 38 cm long. Sixteen cm of coarse brown peat overly 22 cm of dark brown, humified peat. At 38 cm the profile transitions to a bluish gray sand. Charcoal near the base of this section was dated to 3.2 cal ka BP and samples from the middle of the section have younger ages of 0.48 and 0.39 cal ka BP (Table 1). Another sample from the base of the section yielded an age of 0.19 cal ka BP, which anomalously young and likely indicates reworking of material, perhaps by bioturbation, from further up in the sequence.

TØ13-03 is a 37-cm section, ~4 m northeast of TØ-13-02, and further up the slope of the hill (Figure 2). The stratigraphy shows coarse grading to finer brown peat down to 27 cm depth, with humified dark brown peat from 27 to 35 cm and bluish gray sand below 35 cm. The basal date is 3.7 cal ka BP and another date from the middle of the section is 1.4 cal ka BP (Table 1).

TØ13-04 was collected ~4 m northeast of TØ-13-03, also further up the slope of the hill (Figure 2). The stratigraphy is very similar to the previous two sections, although its location higher up on the hill suggests it should be younger. The top 19 cm is coarse to fine brown peat. From 19 to 29 cm is dark brown humified peat, and below this is bluish gray sand and gravel. The basal age is 1.6 cal ka BP (Table 1).

TØ13-05 consists of reddish brown peat above ~30 cm, and dark brown humified peat below this to ~47 cm. All this is underlain by bluish gray sand. Two samples from the base of the section were dated to yield a date of ~3.2 cal ka BP, and an anomalously young age, 0.12 cal ka BP. The first is more stratigraphically consistent with two dated samples from the middle of the section with ages of ~1.2 cal ka BP (Table 1).

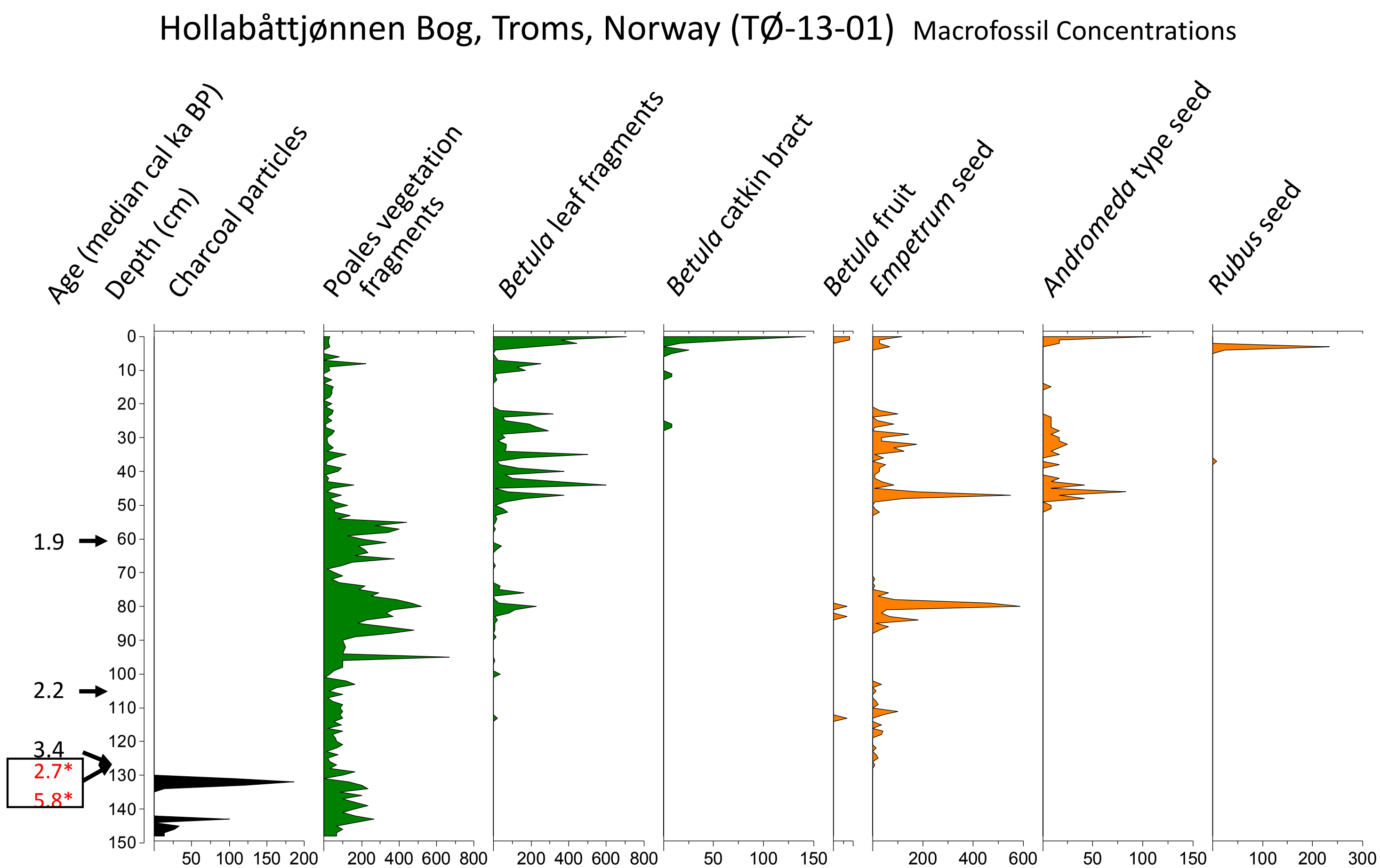

Figure S1. Plant macrofossil and charcoal (>250 µm) concentrations from Hollabåttjønnen Bog recalculated to #'s/100 cc in sediments from peat profile TØ 13-01. Vegetative macrofossils shown in green; propagules in orange. Poales vegetation fragments include both Poaceae and Cyperaceae. Median ages (cal ka BP) rounded to one decimal point. Ages in red with asterisk were rejected as being too old (5.8 cal ka BP) or too young (2.7 cal ka BP).

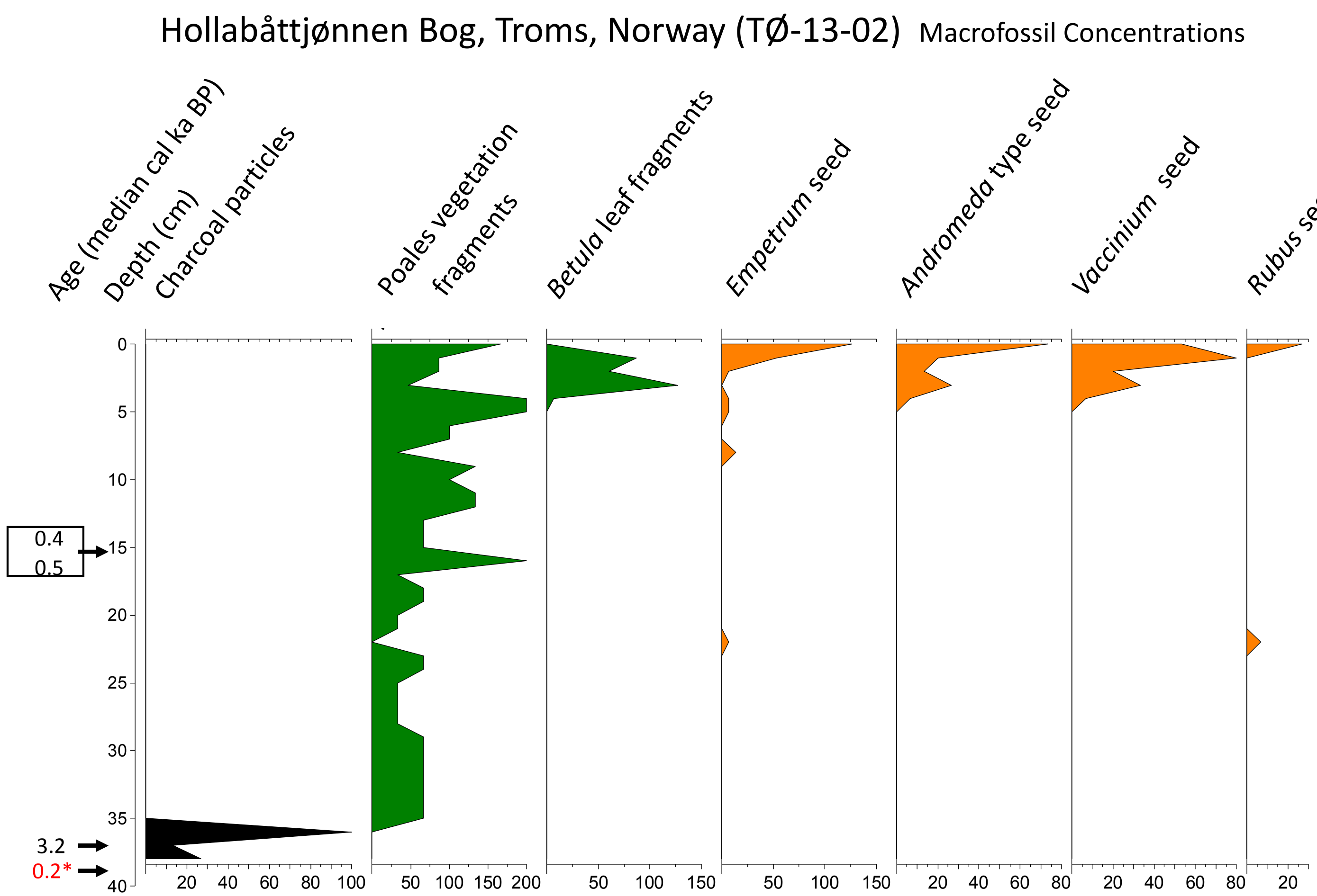

Figure S2. Plant macrofossil and charcoal (>250 µm) concentrations from Hollabåttjønnen Bog recalculated to #'s/100 cc in sediments of peat profile TØ 13-02. Vegetative macrofossils shown in green; propagules in orange. Poales vegetation fragments include both Poaceae and Cyperaceae. Median ages (cal ka BP) rounded to one decimal point. Age in red with asterisk was rejected as being too young.

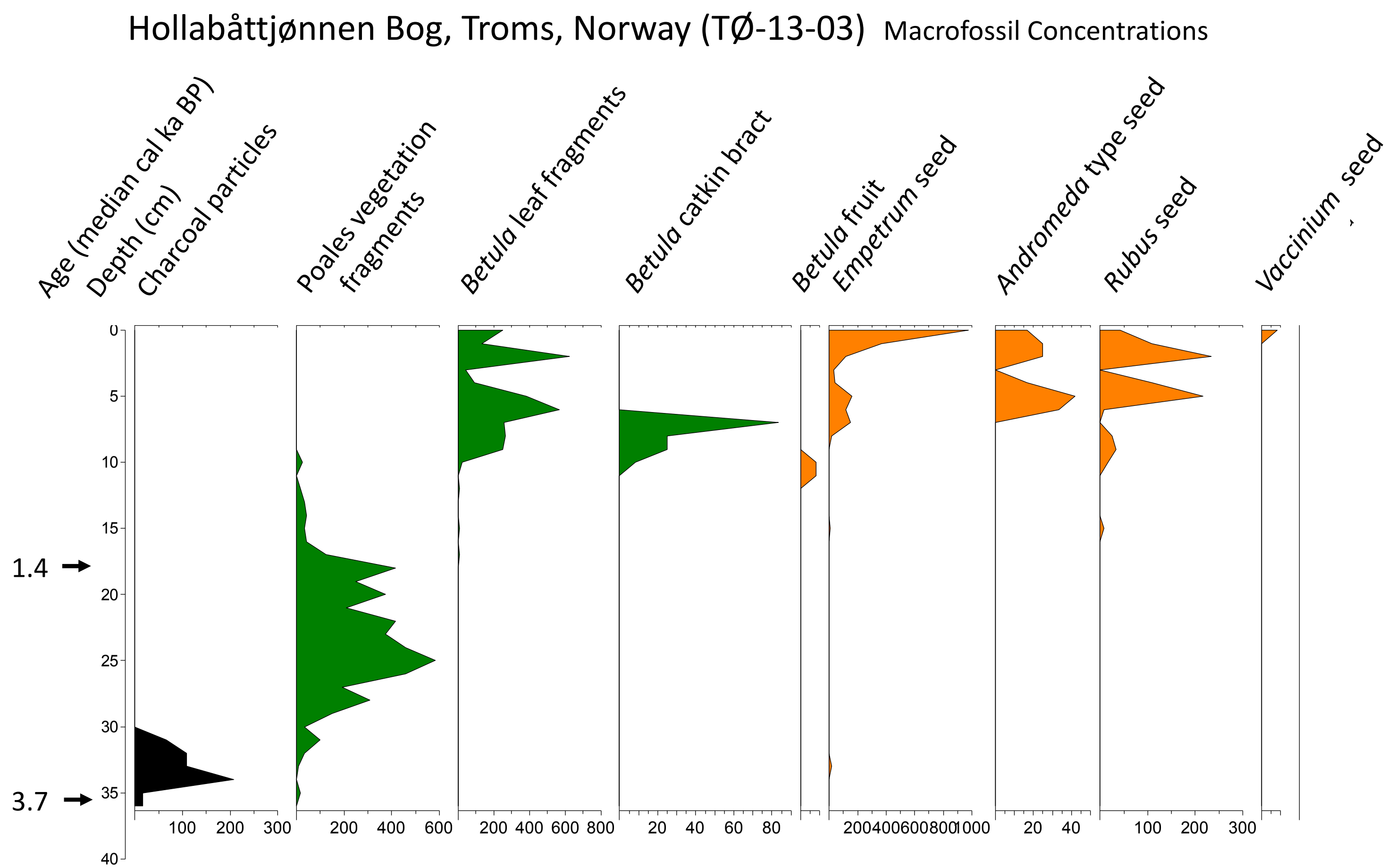

Figure S3. Plant macrofossil and charcoal (>250 μm) concentrations from Hollabåttjønnen Bog recalculated to #'s/100 cc in sediments of peat profile TØ 13-03. Vegetative macrofossils shown in green; propagules in orange. Poales vegetation fragments include both Poaceae and Cyperaceae. Median ages (cal ka BP) rounded to one decimal point.

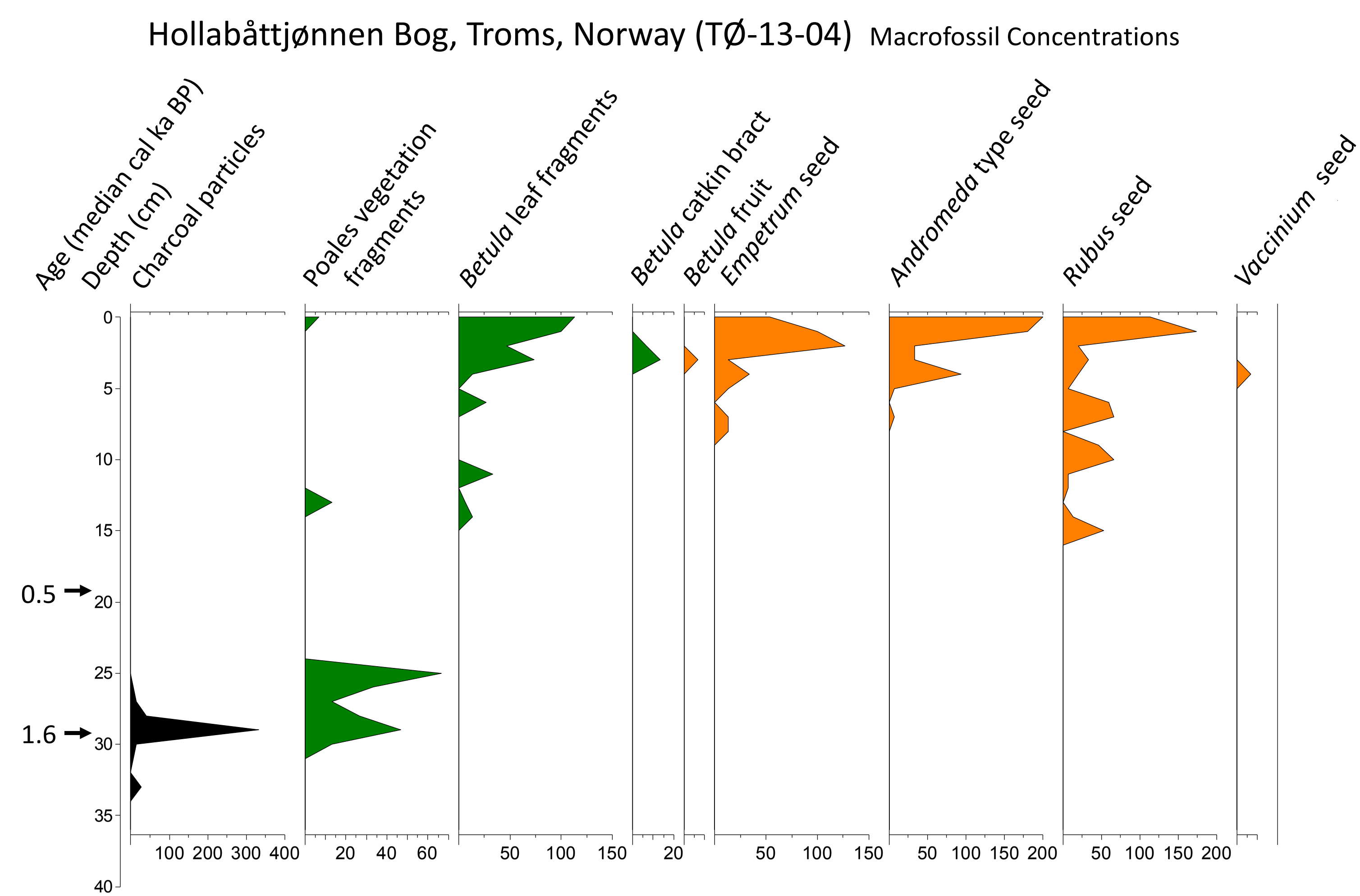

Figure S4. Plant macrofossil and charcoal (>250 µm) concentrations from Hollabåttjønnen Bog recalculated to #'s/100 cc in sediments of peat profile TØ 13-04. Vegetative macrofossils shown in green; propagules in orange. Poales vegetation fragments include both Poaceae and Cyperaceae. Median ages (cal ka BP) rounded to one decimal point.

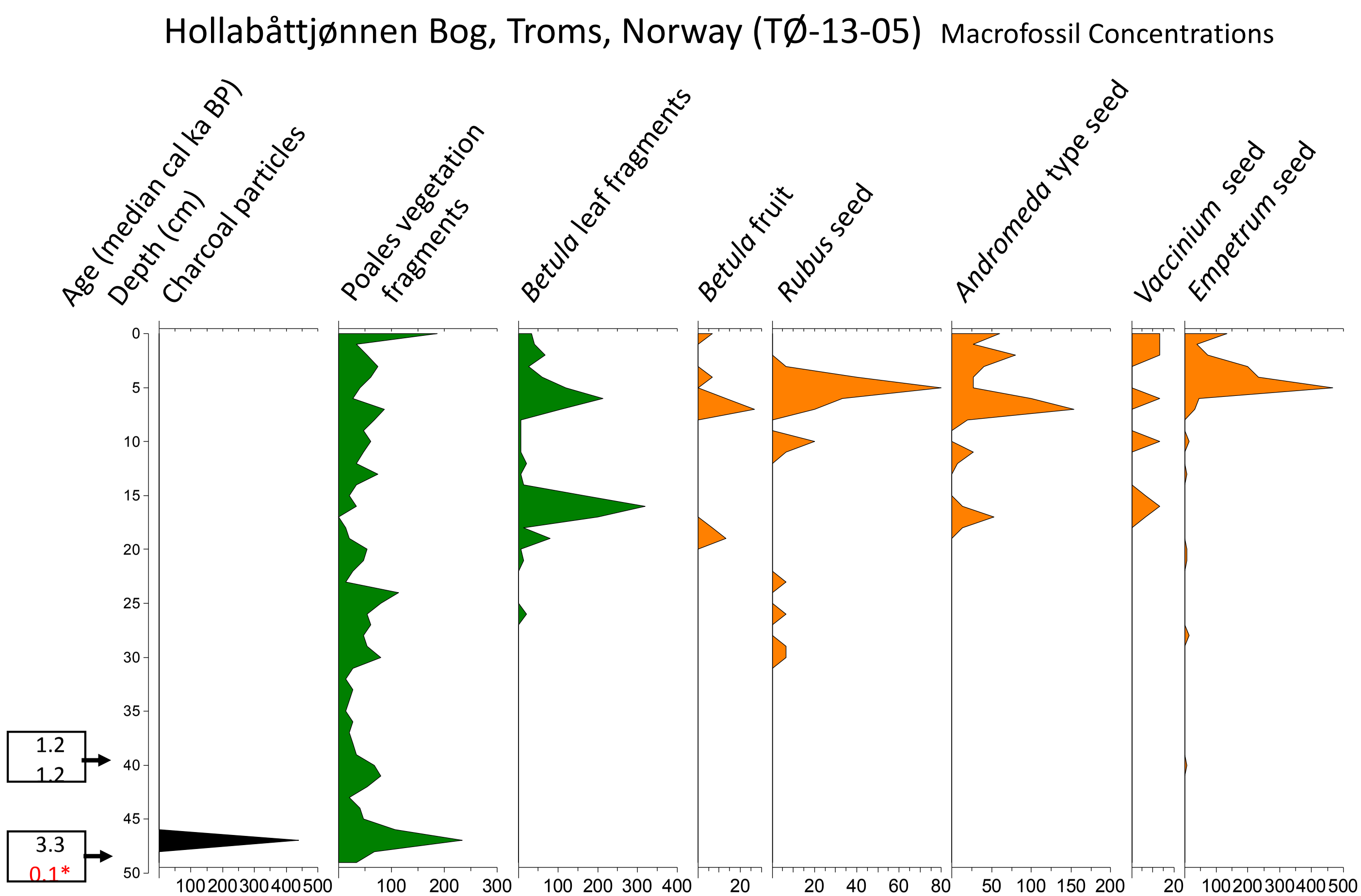

Figure S5. Plant macrofossil and charcoal (>250 µm) concentrations from Hollabåttjønnen Bog recalculated to #'s/100 cc in sediments of peat profile TØ 13-05. Vegetative macrofossils shown in green; propagules in orange. Poales vegetation fragments include both Poaceae and Cyperaceae. Median ages (cal ka BP) rounded to one decimal point; age in red with asterisk was rejected as being too young.